Analyzing Drivers of Compound Coastal Water Events (CCWE) with Copulas:

A Case Study in Eastern North Carolina

By

Kelley De Polt

December, 2021

Director of Thesis: Dr. Scott Curtis

Major Department: Geography, Planning & Environment

Compound Coastal Water Events (CCWE) are a type of multi-hazard climate event characterized by three different types of flooding: Tidal, Fluvial, and Pluvial. To differentiate between these types, tidal is caused by extreme tide conditions, fluvial is caused by rivers or streams overflowing their banks, and pluvial is caused by extreme precipitation. Through an in-depth analysis of the current literature, it does not appear that research has been taken to analyze the relationship between all these drivers.

Eastern North Carolina is a suitable location to research CCWE given its climatologic and research setting. Estuary environments are particularly at risk of compound flooding due to the exposure posed by the geography of river systems meeting the open ocean. Eastern North Carolina is known for having the second largest estuary systems in the United States. Tropical cyclones are often a cause of all three of these CCWE drivers occurring at the same time and location. North Carolina, on average, has a hurricane landfall every 5 to 7 years, and is often impacted by hurricane remnants that make landfall in another state.

When stakeholders prepare for these events the current hazard assessment tools are univariate or bivariate. Examples being floodplain maps primarily considering fluvial flooding and tidal inundation maps predominantly considering tidal flooding. Furthermore, there is little integration of precipitation which represents the pluvial aspects and is actively requested by stakeholders. A more effective approach would be to consider all three components.

This study seeks to further understand the relationship between drivers of CCWE that

occur in Eastern North Carolina. Analyses of three different locations were conducted to determine if there is a regionality of these relationships. The proposed methodology includes two processes. The first is a trivariate copula-based approach using the proxies of precipitation, stream discharge and tidal gauge data for CCWE drivers. The second process is to compare data sourced from a focus group with practitioners who respond and prepare for CCWE.

Through utilization of copula models, simulated CCWE were created to create return periods from an initially limited data set. Trivariate "AND"-based return periods are studied specifically as they quantify the chance that all drivers occur and meet or exceed a certain measurement. All three case studies have statistically similar distributions of trivariate return periods of CCWE though the southern location has a greater amount of lower return period values. Lower return period values indicate a higher probability of occurrence further denoting a higher risk environment.

In interpreting the qualitative data sourced from a focus group consisting of decision makers within Eastern North Carolina, further information about CCWE was revealed building upon the statistical analysis. In the investigation of survey results and transcribed discussions, the decision makers perceptions of the CCWE drivers coincided with the research motivations and copula simulated results, emphasizing the importance of precipitation as an important driver of CCWE. Participants noted how they see the compounding nature of these events within their constituency, and they view that they are at a high level of risk to these events. Combining the physical and social science data provided a better understanding of CCWE from a risk perspective and a decision-making context. Future work could delve into further temporal and spatial scales considering more study locations as well as the seasonality of events. CCWE are a phenomenon that is extremely relevant to vulnerable coastal communities and further understanding of it will be able to benefit those who reside in these regions.

Analyzing Drivers of Compound Coastal Water Events (CCWE) with Copulas: A Case Study in Eastern North Carolina

A Thesis Presented to
the Faculty of the Department of Geography, Planning & Environment
East Carolina University

In Partial Fulfillment
of the Requirements for the Degree
Master of Science in Geography

By
Kelley De Polt
December, 2021

Analyzing Drivers of Compound Coastal Water Events (CCWE) with Copulas:

A Case Study in Eastern North Carolina

By

Kelley De Polt

APPROVED BY:

Director of Thesis _____

Scott Curtis, PhD

Committee Member _____

Burrell Montz, PhD

Committee Member _____

Anuradha Mukherji, PhD

Committee Member _____

Rosasa Ferreira, PhD

Chair of the Department of

Geography, Planning, and Environment _____

Jeff Popke, PhD

Dean of the Graduate School _____

Paul J. Gemperline, PhD

Acknowledgements

I would like to first acknowledge and give thanks to my advisor Dr. Scott Curtis for all the advice and leadership throughout the creation of this thesis project. I am greatly appreciative of the opportunity to continue my studies and work on this impactful project. This project introduced me into the world of multi-hazard research and the importance it has. I hope to participate in this type of research further throughout my career, and I am excited to see where it goes. I would also like to thank Dr. Burrell Montz, Dr. Rosana Ferreira, and Dr. Anuradha Mukherji for their guidance on my thesis committee and providing vital comments and edits.

I would not have been able to accomplish this work without the encouragement by all of my family, friends, and colleagues within the Department of Geography, Planning, and Environment, so I would like to sincerely thank them as well. During the COVID-19 pandemic, which I completed my entire program within, there were many unknowns and changes. Support by all previously mentioned eased many difficulties that may have occurred.

This study was funded by NOAA Coastal and Ocean Climate Applications (COCA)/ Sectoral Applications Research Program (SARP) "Assessing and Communicating Economic Impacts and Risks Associated with Water Resource Management Challenges Along the Coast (joint competition).

Table of Contents

LIST OF TABLES

LIST OF FIGURES

1 INTRODUCTION

Most major weather and climatic events are composed of multiple drivers with compounding effects (Zscheischler et al., 2018). These events can be broadly defined as compound events. One form of compound events that impacts Eastern North Carolina is Compound Coastal Water Events (CCWE). Flooding in coastal regions typically includes three forms: tidal, fluvial, and pluvial. To differentiate between these types: tidal floods occur during exceptionally high tide events. Fluvial flooding occurs when the water levels in a body of water overflow onto the surrounding land. Lastly, pluvial floods occur when extreme rainfall creates a flood independent of an overflowing water body. When all of these flood types occur in the same spatial and/or temporal location, it is defined as a CCWE. Tropical cyclones, such as Hurricane Florence or Hurricane Matthew, are examples of events where all flood types occurred concurrently to result in a CCWE.

In preparation for tropical systems, and their resulting flood impacts, common hazard assessments only account for one driver at a time. For example, flood plain maps used in estimation of flood insurance only account for the fluvial (i.e., river-based) flooding extent. Another hazard assessment approach, maps to assess possible storm surge inundation based upon tropical cyclone intensity, will only assess tidal flooding. There is often little integration between these maps and the additional hazards posed by extreme rainfall. Hazard risk maps of pluvial (i.e., precipitation-based) flooding are actively requested by planners and emergency managers. To prepare and understand compound events, including CCWE, it is important for researchers and practitioners to note drivers do not occur in isolation but are strongly coupled (AghaKouchak et al., 2018) more effectively.

This thesis investigates the relationships between drivers of CCWE using the proxies of extreme precipitation, stream discharge, and tidal height above mean lower low water (MLLW) for three locations in Eastern North Carolina. A methodology which allows trivariate analysis is through the use of copulas which are multivariate distribution functions used

for associating dependence between random variables. Furthermore, content from a focus group will be investigated to determine instances where decision makers referenced aspects of CCWE. The results from the statistical analyses are the compared with the focus group data to determine the extent to which emergency managers and planners in the study region expect and understand the compounding of flood risk in their communities. It is important to determine which variables are particularly worrisome for decision makers. Results will then be conveyed to the focus group participants following the completion of the project. Through being more spatially comprehensive and incorporating meteorological information and social science information to create a mixed methods approach, advancements are made in the scope of risk assessments. Through these analyses a better understanding of CCWE will be revealed, and the following research questions are explored:

1. What is the relationship between tidal, fluvial, and pluvial based flood risk within Eastern North Carolina compound coastal water events?

2. Is there a regionality to the effects of compound coastal water events within Eastern North Carolina?

3. How are perceptions held by decision makers in Eastern North Carolina related to compound coastal water events?

2 LITERATURE REVIEW

This section introduces an overview of previous literature on various topics relating to CCWEs. First, this literature review defines the concepts of hazards, risk, and multi-hazard events. Additionally, the concept of CCWEs is introduced and then related to the study region of Eastern North Carolina. Finally, the last section covers stakeholder approaches currently used in anticipation and response to flood hazards.

2.1 Hazards and Risk

Here some terms used within the risk communication sphere are defined which are referenced throughout this study. First, risk is the likelihood of harm or loss occurring, which is influenced by the environment's exposure and level of vulnerability. Jaeger et al. (2001) also defines risk as a situation or event in which something of human value is put in a vulnerable position and the outcome is uncertain. Risk is related to the concept of uncertainty, as a focus of the quantification of risk is within return periods or probabilities of occurrence. The study and analysis of risk looks at the frequency or chances at which things can go wrong and the expected impacts. The impacts which occur are influenced by hazards and vulnerability of the area and people affected. Hazards are the potential in events occurring and events are the cause of or means by which harm and loss may occur (Tierney, 2014). Another term, resilience is something which needs to be considered together with the concept of risk, as both risk and resilience arise from social orders and structures. Resilience is the ability for social entities to manage the impacts of events and recover quickly. This includes coping, adapting, and recovering from events (Tierney, 2014). In summary, risk is the likelihood of harm or loss from a hazard. Areas at risk may feel a greater impact depending on their level of vulnerability and resilience.

2.2 Multi-Hazard Events

When adverse events take place, it is not common that only one hazard or driver occurs. It is important in the consideration of mitigating impacts of these events to realize the multivariate aspects as several non-independent variables may be of interest (Salvadori et al., 2016). Multi-hazard events can include compounding, cascading, and consecutive hazards. Each of these requires a different approach to research methods.

Compound events can be defined as (1) two or more extreme events occurring simultaneously or successively; (2) the combination of extreme events with underlying conditions that amplify the impact; or (3) a combination of events that are not themselves extreme but lead to an extreme event when combined (Sadegh et al., 2018). Compound weather and climate events have four themes: preconditioned, multivariate, temporally compounding, and spatially compounding (Zscheischler and Fischer, 2020). Impacts from a compound event depend on the nature and number of hazards, the spatial and temporal locations, the relationships between the hazards, and perspectives of stakeholders involved (Leonard et al., 2014).

In the scope of multi-hazard climate events, they are composed of climatic and weather phenomenon-based drivers that may span similar spatial and temporal scales. It has been recognized within the literature that most major weather and climate-based events are caused by compounding effects of multiple hazards (Zscheischler et al., 2018). The combination of multiple climatic drivers contributes to both societal and environmental impacts. The impacts of these events can be mainly due to one of the drivers being in an extreme state, though it is more common that the combination of the drivers which may not be in an extreme state led to an extreme impact.

A challenge with understanding and anticipating compound events is that the relationships between hazards or drivers can make the estimation of event probability and intensity more difficult as opposed to considering all separately. Though if the drivers are not con-

sidered together, that may lead to an underestimation of risk. In accounting for all drivers and their dependencies a better understanding of their nature and predictability will arise. Identifying the dependencies between the different hazards is an important aspect in the study of these events (Zuccaro et al., 2018).

There are numerous reasons why compound events have come to the attention of the hydrologic and climatic communities. One reason is the rising awareness of the non-stationarity of the climate system, which also means the need to better understand interactions between drivers of events (Leonard et al., 2014). Another reason is the argument for a paradigm shift to incorporate compound events into climate impact analysis. This can be done by embedding these events into the general risk framework: the linkage between hazards, vulnerability, and exposure. Using an impact-centric perspective in a risk framework allows guidance for identifying the most relevant hazards. A risk framework is not the only framework which will need adoption. This consideration of compound events will also lead to a new climate research analysis framework where hazards will need to be considered with all drivers considered together (Zscheischler et al., 2018). By knowing the relationships of processes driving compound events and the probabilities of occurrence, mitigation of these high-impact events can be improved (Wahl et al., 2015).

2.3 Floods in Coastal Settings

A flood is the overflowing of the normal confines of a stream or other body of water, or the accumulation of water over areas that are not normally submerged. Floods include river (fluvial) floods, flash floods, urban floods, pluvial floods, sewer floods, coastal floods, and glacial lake outburst floods. In coastal regions, flooding is a compound event primary caused by sea sources, inland sources, and if close to a river there could be river sources (Archetti et al., 2011).

2.3.1 Fluvial Floods

Fluvial floods, also known as flood plain flooding, riverine flooding, or over-topping banks, occur when the capacity of a river or stream is exceeded. There are seasonal and intra-annual variations in river flow resulting in extremely high flow periods, though fluvial floods are mainly influenced by excess rainfall within the river's basin (Karamouz et al., 2013). This rainfall can result in rivers rising, even if the rains are farther up the watershed. A river's response to rainfall is dependent on characteristics of the rainfall and the river itself, an example being the rise and fall rate in larger rivers is much slower than in smaller rivers (Karamouz et al., 2013).

2.3.2 Pluvial Floods

Pluvial flooding is a type of flooding caused by precipitation. It can also be known as storm water, flash flooding, or ponding. Pluvial flooding is common within flat areas where the runoff produced exceeds the storage capacity of the ground, canals, lakes, or other infrastructure. In this type of pluvial flooding puddles or ponding on land. Sources of precipitation include smaller-scale precipitation systems such as storm scale or mesoscale systems (Teegavarapu, 2012). A type of storm scale system is an isolated thunderstorm which can cause local flash flooding from heavy localized rainfall. Mesoscale systems are not as isolated as storm scale systems. They are more organized into lines or bands or into clusters of individual storms causing broader flash flooding. Tropical systems can be seen as a mesoscale system (Hirschboeck et al., 2000).

2.3.3 Tidal Floods

Tidal flooding may also be known as king tide, storm surge, high tide, or coastal flooding. Extreme high tide alone is able to cause widespread coastal flooding (Castrucci and Tahvildari, 2018). Sea surge is defined within the meteorologic sphere as the difference in

water level between the observed sea level and the predicted astronomical tide. Storm surge is typically caused by water carried by storm winds toward the coast. These storm winds are accompanied with tropical cyclones causing both long and short-wave surges that affect the open ocean, bays, rivers, streams, inlets, and low-lying land near the sea (Karamouz et al., 2013). Storm surges are the main cause of coastal flooding which can lead to multiple adverse impacts such as loss of human lives, damage to infrastructure, and disruption of industry (Resio and Westerink, 2008).

2.3.4 Compound Coastal Water Events

Within coastal environments flooding drivers are strongly interconnected. These drivers may include river flow, precipitation, coastal water level, surge, and wind speed. Considering precipitation and tidal conditions together, when high tidal levels and heavy precipitation co-occur, the potential for flooding in low-lying areas is greater than in isolation. Research has shown that sea level rise has caused the increase in minor flooding events composed of the drivers of high tides and precipitation (Ezer and Atkinson, 2014). Precipitation also increases the flood risk at river confluences (Zscheischler et al., 2018). Its contribution can be especially seen in the river tributaries that then amplify the mainstream flow (Chen et al., 2012). Other factors which can play a role in creating impactful flood events include topography and land cover types. In other portions of river basins, such as the tidal regions also known as estuarine environments, flooding can occur because of high river flow, high sea levels, or the combination of the two (Buschman et al., 2019). Compound flooding hazards might be exacerbated in the future due to the effects of climate variability on sea level rise (Wahl et al., 2015; Bevacqua et al., 2019).

The combination of all these drivers makes coastal areas especially vulnerable to flooding. The combination of all these drivers also makes this event a CCWE. Tropical cyclones are prime examples of all these flood sources being produced concurrently. Precipitation associated with the cyclone may subsequently result in river runoff, while the low pressure

at the center may act to raise the tidal level.

Recent approaches to study aspects of compound flooding include the analysis of compound flooding in estuaries from river discharge and storm surge with multiscale modeling approach (Olbert et al., 2017; Kumbier et al., 2018), the drivers of precipitation and river discharge using a 2-dimensional copula approach (Apel et al., 2016), using an analysis of levee performance under fluvial (i.e., stream) and pluvial (i.e., precipitation) floods using bivariate scenarios and stress-flow models (Jasim et al., 2020), storm surge and precipitation on a continental and global scale (Wahl et al., 2015; Bevacqua et al., 2019), and lastly the hazards from river discharge and storm surge drivers at a global scale (Couasnon et al., 2020). Though to our knowledge there has not been a study involving the drivers pluvial, fluvial, and tidal within the same analysis.

There is no set mathematical approach to defining CCWEs through multiple statistical approaches have been performed. The common methodology includes examining the dependence between proxy variables of flood hazard types (Bevacqua et al., 2019; Hendry et al., 2019; Kew et al., 2013; Sadegh et al., 2018; Svensson and Jones, 2002, 2004; Wahl et al., 2015; Ward et al., 2018; Wu et al., 2018; Zheng et al., 2013). Similar to this study recent studies have used copulas to characterize the bivariate joint distribution and dependence (Bevacqua et al., 2019; Ward et al., 2018).

2.3.5 Historical Flood Events in Eastern North Carolina

Within a span of twenty years, Eastern North Carolina has been impacted by three devastating tropical cyclone-driven floods: Hurricanes Floyd, Matthew, and Florence, which caused major impacts to water quality, biogeochemistry, and ecological conditions (Paerl et al., 2019). October 8th, 2016, Hurricane Matthew made landfall in South Carolina as a category 1 after a gradual decline from a category 5 classification (Stewart, 2017). Extreme rainfall and flash flooding ensued within this storm given the occurrence of an extratropical transition and pre-existing frontal boundary which amplified precipitation totals north of

the center of the system. Matthew broke many precipitation records set in Eastern North Carolina during Hurricane Floyd, which made landfall in North Carolina on September 16th, 1999 (Pasch et al., 1999). Nearly two years later, on September 14th, 2018, Hurricane Florence made landfall in North Carolina as an upper-level category 1 storm (Stewart and Berg, 2019). Freshwater flooding and storm surge were the primary hazards during this storm, these being amplified by large precipitation totals. Florence exceeded Matthew's precipitation totals, specifically within a narrow swath of rainfall amounts exceeding 30 inches. Given these most recent extreme occurrences, there has been a focus of research on impacted communities and how they should mitigate and respond to extreme flood events. In an analysis of rainfall records for Coastal North Carolina since 1898, there was a period of unprecedentedly high precipitation since the late-1990's coinciding with these three events. In the same study over the past 120 years there has been a trend toward increasingly high precipitation associated with tropical cyclones (Paerl et al., 2019). This regime shift could have major ramifications for hydrology, water quality, and flooding impacts.

2.4 Approaches to Flood Risk

2.4.1 Hazard Maps

Flood hazard or risk maps are important as precautionary measures as they serve as a basis for spatial planning, local hazard assessment, emergency planning, and technical protection measures (CITATION). There are different requirements and needs from various user groups to be achieved by flood maps and web mapping services. One source of these maps includes web services, which convey flood information which allows users to examine flood extents and corresponding water depths along with real time gauge levels. In the United States, common flood hazard assessment practices typically account for one driver at a time, an example being either fluvial flooding (Alfieri et al., 2014; Dottori et al., 2016; Hirabayashi et al., 2013; Ward et al., 2013, 2017; Winsemius et al., 2013, 2016) only or ocean

flooding only (Brown et al., 2016; Hinkel et al., 2014; Muis et al., 2016; Vousdoukas et al., 2018). Similarly, flood hazard mapping procedures for coastal water levels do not account for factors such as river discharge or localized precipitation (Moftakhari et al., 2017). One hazard assessment, regulatory flood hazard maps only model flooding with one of these drivers (Federal Emergency Management Agency, 2020; Moftakhari et al., 2019) which causes an inaccurate representation of flood hazard.

2.4.2 Stakeholder Flood Response

Emergency management can be defined as an effort to plan how to deal with disasters in the most effective manner. Traditionally, emergency managers have confined their activities to developing emergency response plans and coordinating the initial response to disasters (National Research Council, 2011). This suggests that the profession is in charge of administrative decisions and actions that anticipate events, reduce vulnerability, and address the impacts of disasters. Emergency management is therefore related to many other professions and areas of employment including but not limited to risk management, business continuity planning, land-use planning, flood plain management, emergency services, homeland security, and humanitarian assistance. Emergency management directors will be needed to develop response plans to protect more people and property, and to limit the damage from emergencies and disasters (McEntire, 2018). As the role of the emergency manager evolves to address risk in all emergency management phases, emergency managers need tools to understand how to assess hazards and reduce vulnerability (National Research Council, 2012).

Emergency planning is defined as a cycle of planning, training, exercising, and revision that continues throughout the five phases of the emergency management cycle which include preparedness, prevention, response, recovery, and mitigation (Blanchard, 2018). One purpose of the planning process is to develop and maintain an up-to-date Emergency Operation Plan (EOP). The key parts of an EOP assign responsibility to organizations and individuals for

carrying out specific actions at projected times and places in an emergency that exceeds the capability or routine responsibility of any one agency. Emergency planning is a team effort and requires collaboration with personnel from other agencies and organizations. Building an effective team takes time and effort as members go through several stages (Blanchard, 2018).

There has been a massive paradigm shift in flood risk management regarding the responsibility of the governing structure to both the governance and the public. The public has historically placed their trust in public protection measures. This perception can lead to the individual not taking actions for preparedness. Risk communication has broadened focus to include not just information but also awareness. Flood risk communication is an important aspect of flood protection for at-risk communities. The way flood risk is conveyed to these communities has many forms, encompassing both one-way and two-way systems of communication. Sharing accurate information regarding floods is incredibly important. If risk is underestimated, then there may not be as much preparedness prior to an event or for recovery.

2.5 Summary

Compound climate events are multi-hazard events where multiple climatic events occur simultaneously, amplify each other's underlying conditions, or combine to create an extreme impact. The study of compound events is important because ignoring one of the hazards could lead to a misunderstanding or underestimation of impacts that could occur. One example of a compound event is a CCWE, which is the co-occurrence temporally and/or spatially of pluvial-based, fluvial-based, and tidal flooding. Understanding CCWE is extremely important within Eastern NC given historical flooding impacts caused by Hurricanes Floyd, Florence, and Matthew. Hurricanes are an example of a source of all three CCWE flooding drivers occurring. In preparation of Hurricanes, decision makers analyze and share with their constituent's flood hazard or risk maps. These maps typically consider at most two of the

drivers which compose CCWE. In the examples of Hurricanes Florence and Matthew, which occurred 2 years to each other, communities in central and eastern NC experienced flooding 26% larger than their 100-year floodplains (i.e., 10% chance of being exceeded in any one year) (Schaffer-Smith et al., 2020). Not predominantly featured within these hazard assessments is the aspect of precipitation which was important in both of these tropical systems. Another contributing factor to CCWE occurring within Eastern NC is the geographic setting. The combination of occurrence of Hurricanes as well as geographic setting establishes Eastern NC as a prime location to analyze CCWE.

3 DATA AND METHODOLOGY

This chapter presents the study region, data sets utilized, and methods for both statistical analysis and qualitative data analysis The study region encompasses three regions within Eastern North Carolina (i.e., northeastern, central eastern, and southeastern). The section on data acquisition and description details the proxies for drivers of CCWE and where to obtain them. The section on statistical analysis details the copula model methodology and arrangement of a stakeholder focus group.

3.1 Study Region

The proposed methodology for studying CCWE is utilized for the study region of Eastern North Carolina (NC), United States. Eastern NC has a humid subtropical climate. NC encounters the hazards of tropical cyclones, droughts, heat waves, severe storms, and winter weather. One of the hazards which most directly impacts Eastern NC and is one of the motivating factors of this research, is tropical cyclones also known as hurricanes or tropical storms. On average the state encounters a hurricane landfall every 5 to 7 years (NOAA National Hurricane Center, 2021).

The hydrologic and geographic setting of Eastern NC is characterized by relatively flat terrain, which makes it vulnerable to many natural hazards, especially that of flooding. Eastern NC is also known for having the second largest estuary system within the United States composing of 5,432 kilometers of non-oceanfront shoreline (Bulla et al., 2017). These estuarine environments are at particular risk to CCWE given the intersection of riverine flow and ocean tides (Olbert et al., 2017).

Within the study region, three case study locations (i.e., northern, central, and southern) are selected based upon station availability. The limiting factor to selection of case study locations was the availability of tidal gauges that encompassed the desired period of record. The northern case study area encompasses two river basins: the Roanoke River basin and

Pasquotank River Basin (Figure 3.1a). These two basins encompass an area of 4,389,964 acres (Pasquotank: 2,154,534 acres; Roanoke: 2,235,430 acres) with 4,213 miles of streams and rivers within. Next, the central case study also comprised two river basins: Neuse River Basin and White Oak River Basin (Figure 3.1b). Together these basins cover an area of 4,763,929 acres (Neuse River: 3,879,756 acres; White Oak River: 884,173 acres) along with containing 3,729 miles of streams and rivers. Lastly, the southern case study is entirely within the Cape Fear River Basin (Figure 3.1c). This basin has a size of 5,864,701 acres with 6,584 miles of streams and rivers.

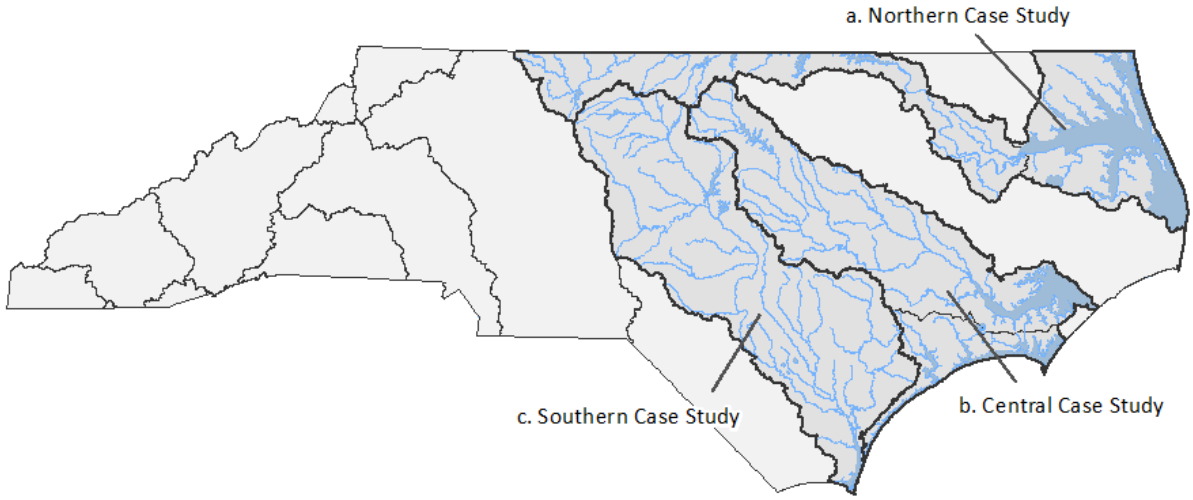

Figure 3.1: Location of case study areas in Eastern North Carolina.

3.2 Data

Compound Coastal Water Event (CCWE) risk is assessed through proxy variables representing the three flood drivers. Precipitation represents pluvial flooding, stream discharge represents fluvial flooding, and water level above MLLW represents tidal flooding. These proxy variables are common in the literature studying compound flooding (Khanal et al., 2019; Klerk et al., 2015; Svensson and Jones, 2002; Ward et al., 2018).

All in-situ station data was retrieved with a temporal record of at least 30 years. There

were only three tidal stations within Eastern NC that fit this criterion and will dictate the regions of analysis. Descriptive information regarding the stations for all counties can be found in tables 3.1, 3.3, and 3.5. Basic statistical information for the three flood proxy variables is given in tables 3.2, 3.4, and 3.6

3.2.1 Precipitation

24-hour precipitation accumulation, the proxy variable for pluvial flooding, was retrieved using the National Oceanic and Atmospheric Administration (NOAA) National Centers for Environmental Information (NCEI) API (https://www.ncei.noaa.gov/support/access-data-service All precipitation stations utilized are part of the Global Historical Climatology Network (GHCN), NOAA's primary station dataset.

3.2.2 Stream Discharge

Mean daily stream discharge (meters cubed per second; m3/s) was sourced from the United States Geological Survey's (USGS) Daily Values Site Web Service (https://waterservices.usgs.gov/rest/DV-Service.html). Stream discharge is the measurement of the quantity of water passing a location along the stream calculated by multiplying the area by velocity (Figure 3.2).

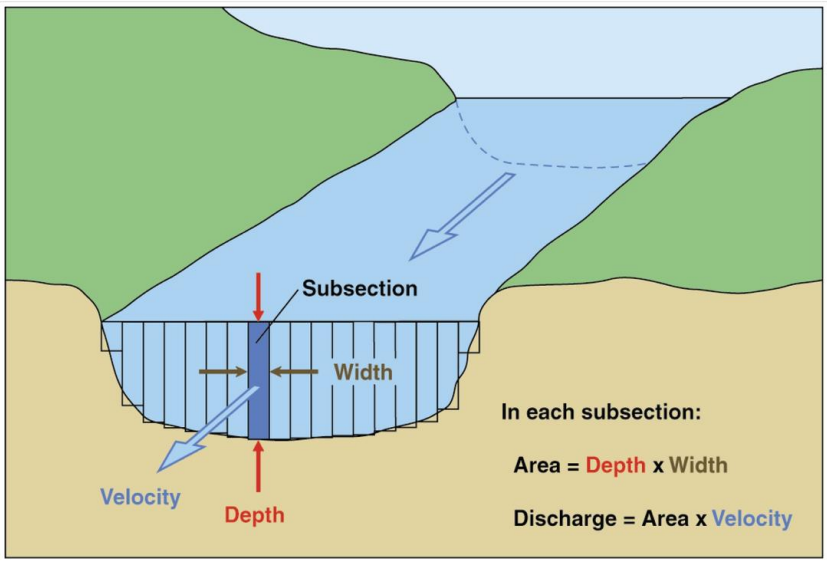

Figure 3.2: Diagram of stream channel cross section with subsections and equations. From USGS.

3.2.3 Tide Level

Water level with the tidal datum of Mean Lower Low Water (MLLW) sourced from NOAA/NOS/CO-OPS stations (Figure 3.3) is used to represent tidal floods. The tidal datum is a standard elevation defined by a phase of the tide. Datums are used as a reference to discuss heights or depths, it could also be seen as a starting point of where to measure from (Figure 3.4). MLLW is the average of the lower low water height of each tidal day observed over the NOAA National Ocean Service Tidal Datum Epoch (1983-2001). This data was retrieved through NOAA Tides and Currents API (`https://api.tidesandcurrents.noaa.gov/api/prod/`).

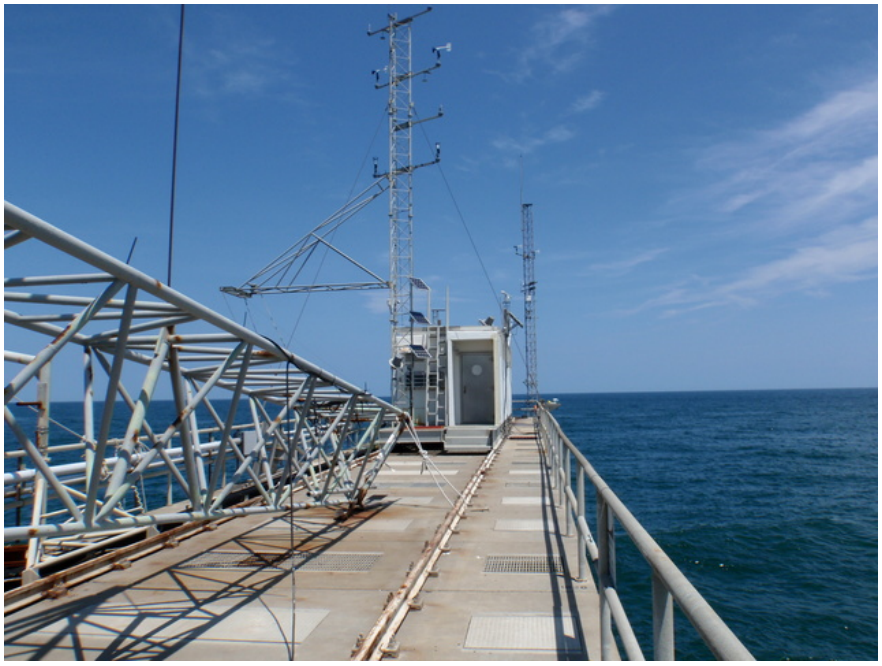

Figure 3.3: Example of tidal gauge station at Duck, North Carolina. From NOAA Tides and Currents.

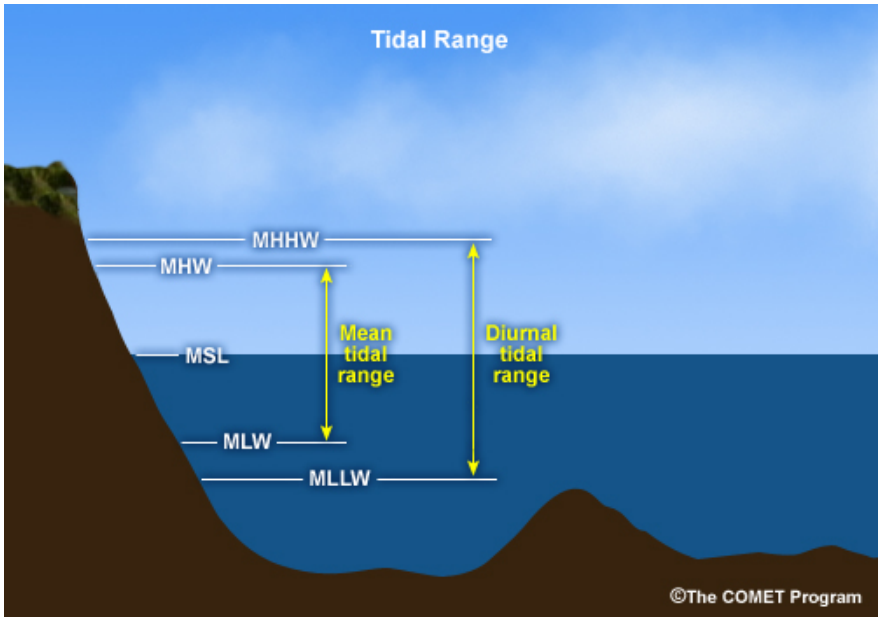

Figure 3.4: Visualization of Tidal Datums. From COMET MetEd.

3.2.4 Selection of Stations

For each of the three study areas (i.e., northern, central, and southern) within the greater study region a triplet of stations is created. A station triplet includes one precipitation station, one stream gauge station, and one tidal station. Through a R script, all possible station triplets are created and the one with the most correlation is selected as the station triplet for that area.

For the northern study area, the station triplet is composed of the precipitation station Edenton, NC, US; the stream discharge station Cashie River at SR1257 Near Windsor, NC; and the tidal station Duck, NC (Figure 3.5). Further station descriptors can be found in Table 3.1 and basic statistics can be found in Table 3.2.

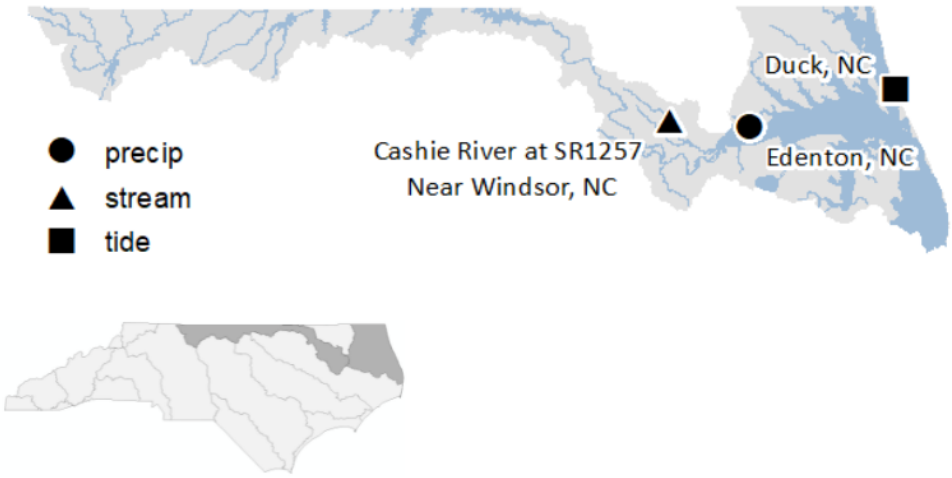

Figure 3.5: Selected Stations within the Northern Case Study.

Table 3.1: Northern Case Study: Station Descriptors

Variable	Station Name	Station ID	Start Date	End Date
Precipitation	Edenton, NC, US	USC00312635	1872-01-01	Current
Tide	Duck, NC	8651370	1979-11-01	Current
Stream	Cashie River at SR1257 Near Windsor, NC	0208111310	1987-06-03	Current

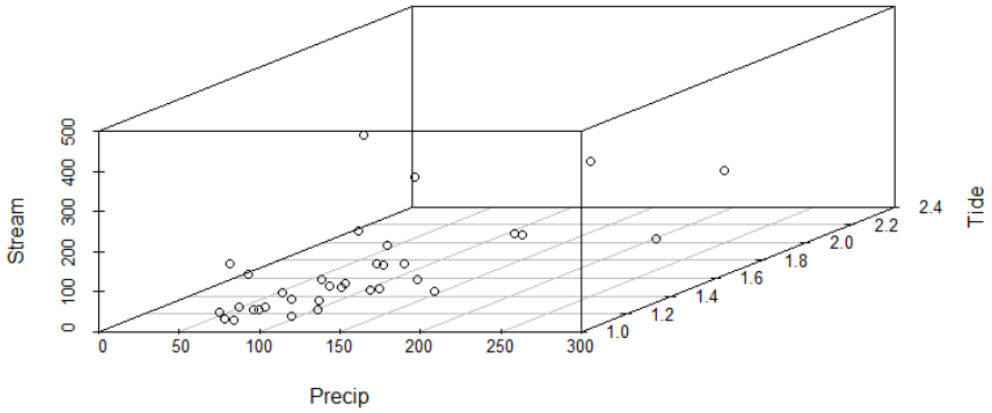

Figure 3.6: Scatterplot of in-situ station measurements for each annual CCWE in the Northern Case Study.

Table 3.2: Northern Case Study: Station variable characteristics

Variable	Minimum	Mean	Maximum	Standard Deviation	Variance	Skewness	Kurtosis
Precipitation	48.30	99.84	274.60	50.84	2584.41	1.66	5.89
Tide	1.12	1.46	2.38	0.28	0.08	1.50	5.42
Stream	0.00	53.67	410.59	93.99	8834.32	2.43	8.54

For the central study area, the station triplet is composed of the precipitation station Trenton, NC, US; the stream discharge station Trent River Near Trenton, NC; and the tidal station Beaufort, NC (Figure 3.7). Further station descriptors can be found in Table 3.3 and basic statistics can be found in Table 3.4.

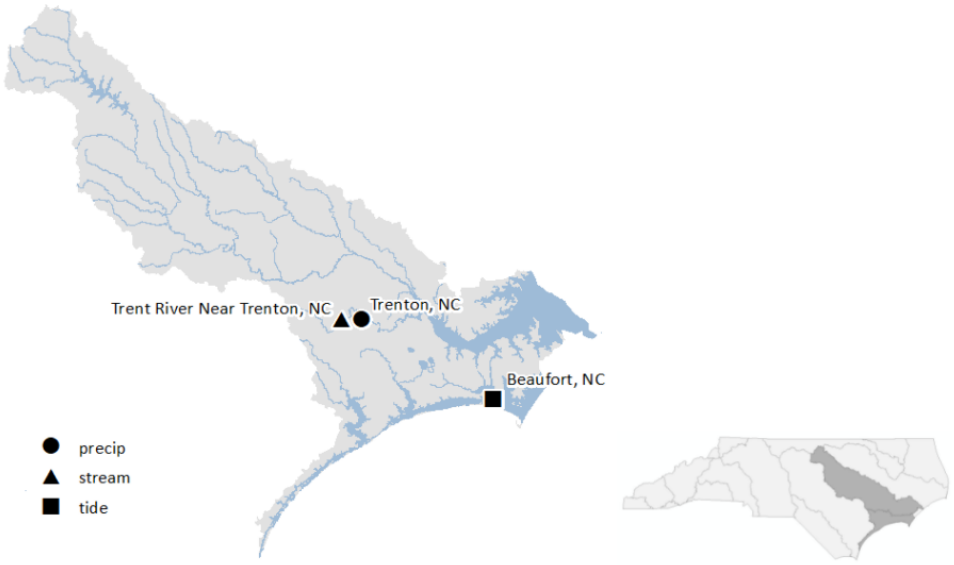

Figure 3.7: Selected Stations within the Central Case Study.

Table 3.3: Central Case Study: Station descriptors

Variable	Station Name	Station ID	Start Date	End Date
Precipitation	Trenton, NC, US	USC00318706	1955-10-18	2014-10-31
Tide	Beaufort, NC	8656483	1979-06-01	Current
Stream	Trent River Near Trenton, NC	02092500	1985-10-01	Current

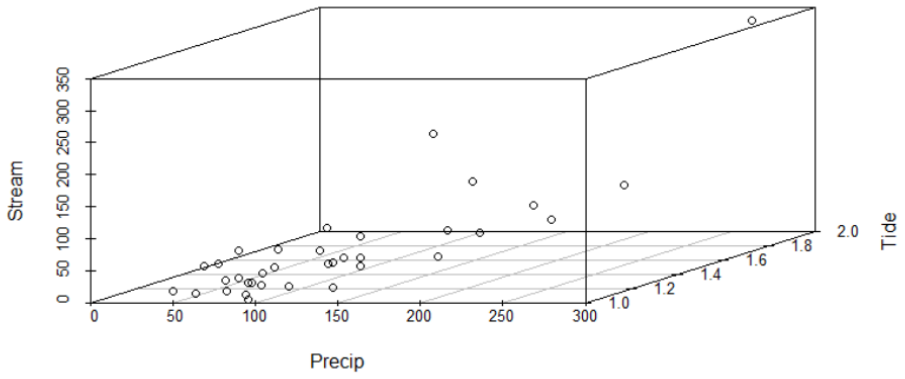

Figure 3.8: Scatterplot of in-situ station measurements for each annual CCWE in the Central Case Study.

Table 3.4: Central Case Study: Station variable characteristics

Variable	Minimum	Mean	Maximum	Standard Deviation	Variance	Skewness	Kurtosis
Precipitation	47.00	103.03	273.60	52.32	2737.13	1.60	5.68
Tide	1.02	1.34	1.92	0.25	0.06	0.87	2.76
Stream	0.14	45.74	339.80	69.03	4764.55	2.84	11.54

For the southern study area, the station triplet is composed of the precipitation station Elizabethtown, NC, US; the stream discharge station Cape Fear at Lock #1 N R Kelly, NC; and the tidal station Wilmington, NC (Figure 3.9). Further station descriptors can be found in Table 3.5 and basic statistics can be found in Table 3.6.

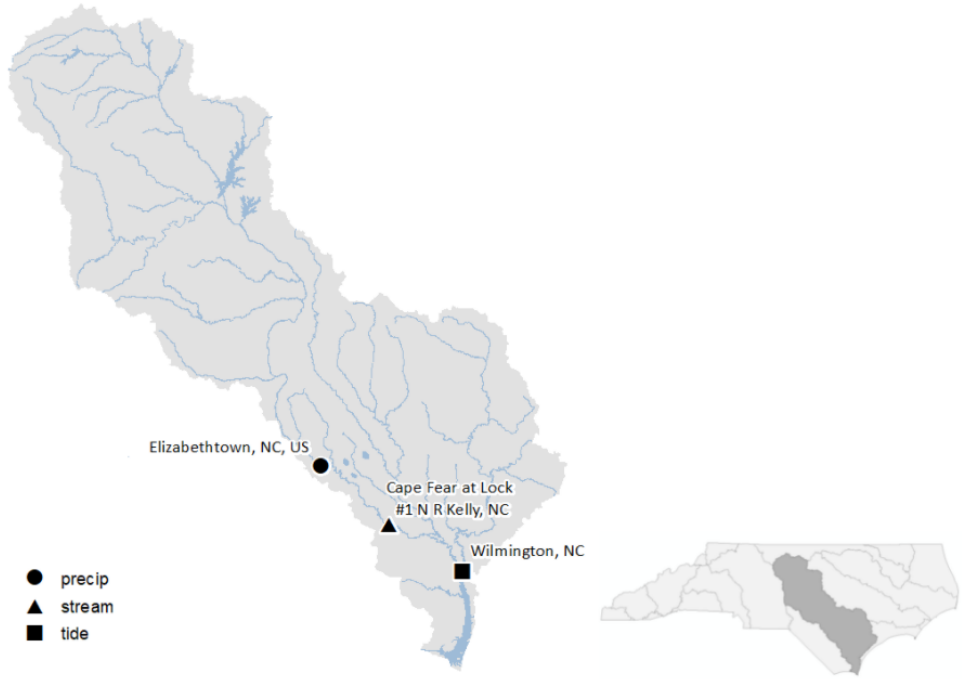

Figure 3.9: Selected Stations within the Southern Case Study.

Table 3.5: Southern Case Study: Station descriptors

Variable	Station Name	Station ID	Start Date	End Date
Precipitation	Elizabethtown, NC, US	USC00312732	1910-12-01	2021-02-27
Tide	Wilmington, NC	8658120	1979-08-31	Current
Stream	Cape Fear at Lock #1 N R Kelly, NC	02105769	1985-10-01	Current

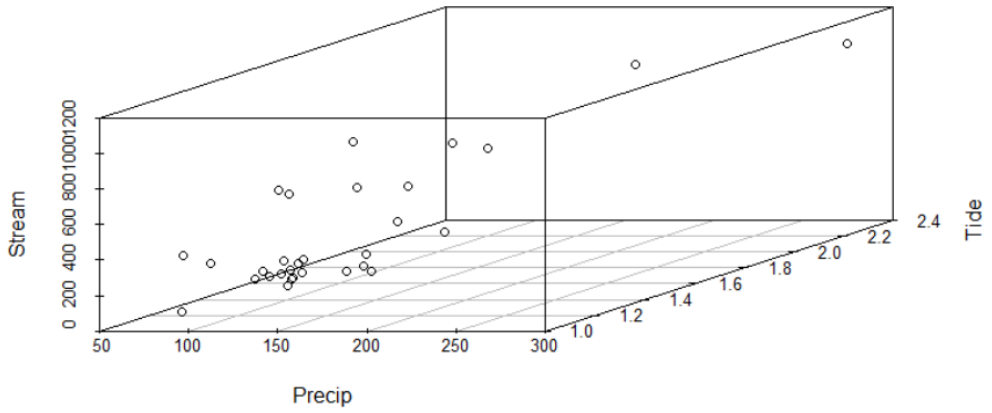

Figure 3.10: Scatterplot of in-situ station measurements for each annual CCWE in the Southern Case Study.

Table 3.6: Southern Case Study: Station variable characteristics

Variable	Minimum	Mean	Maximum	Standard Deviation	Variance	Skewness	Kurtosis
Precipitation	56.10	99.16	298.50	46.25	2138.88	2.97	13.03
Tide	1.19	1.64	2.23	0.25	0.06	0.68	2.95
Stream	20.25	279.67	1067.55	286.51	82087.27	1.37	4.02

3.3 Methods

3.3.1 Designing Compound Coastal Water Events

In this study, the block (annual) maxima approach is used to characterize a CCWE. This approach may also be called the Annual (Maximum) series or AM approach. Within this approach the observational period is divided into non-overlapping periods of equal size and the attention is focused on the maximum observation in each period (Gumbel 1958). The annual maxima observation is the 24-hour accumulation of precipitation. This variable is thought to have the strongest relationship to the other two variables: stream discharge and tide height. After determining the annual maxima 24-hour precipitation accumulation for each year of analysis, the stream discharge and tidal height maxima within three days were found. All CCWE events are listed in Appendix A. Together all three variables are defined as one CCWE in that year. Using a script in R, for each year of analysis.

3.3.2 Copulas

When researching extreme events, multivariate analysis allows for a better understanding of the risk and impacts through considering more than one variable which influences the event. Typically, multivariate frequency distributions have been derived using one of these fundamental assumptions (Zhang and Singh, 2006, 2007): the variables each have the same type of distribution; the variables are assumed to have or are transformed to have a joint normal distribution; or the variables are assumed to be independent. Though in real applications, the variables which make up extreme events are generally dependent, do not follow the normal distribution, and do not have the same type of marginal distributions. One way to undertake multivariate analysis which does not fall to these assumptions is through copula modeling.

A copula is a statistical technique used to connect multivariate probability distributions through the univariate probability distributions (Nelsen, 2006; Salvadori et al., 2016). The etymology of the term copula is derived from the Latin verb "copulare" which means "to join together". Another way to view copulas is as a mathematical function that "joins" or "couples" the best fit univariate distributions (Genest and Favre, 2007). Copulas provide a systematic way of studying the underlying dependence structure and a foundation for constructing families of multivariate distributions (Joe 1997). The advantages of implementing a multivariate copula model are numerous, especially the aspect that each variable in the analysis can be represented by a distribution which represents it best.

The copula method was first developed for use in the fields of statistics and finance by Sklar (1959), with the formulation of their theorem called the Sklar theorem which established the theoretical framework for the copula theory utilized today. Other contributors to copula theory include Joe (1997) and (Nelsen, 2006) who further discussed the dependence structure of multivariate random variables.

In general, the steps of modeling a copula include fitting marginal distributions, model

parameter estimation, goodness-of-fit tests, and model simulations (Favre et al., 2004). The first step fitting marginal distributions is discussed in Section 3.3.3. After determining the best fit marginal distribution for each variable of analysis as well as dependence between the variables (Section 3.3.4), the next step in the copula modelling approach is the selection of appropriate copula and goodness-of-fit testing (Figure 3.11).

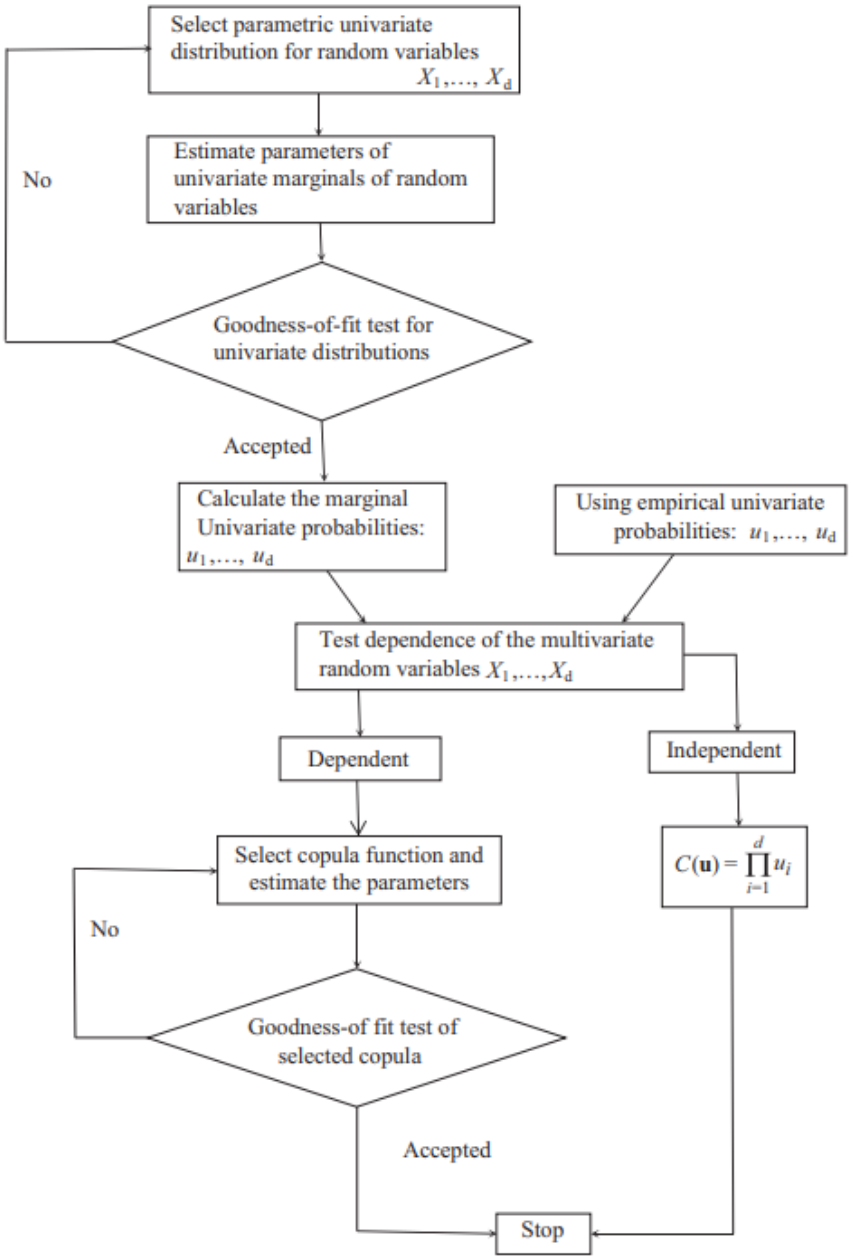

Figure 3.11: Procedure for multivariate frequency analysis via copulas. From Zhang and Singh (2019).

Properties of copulas are explained by Favre et al. (2004) and further discussed in Nelsen (2006) and Joe (1997). Based upon Sklar's theorem, the theoretical foundation, copulas have two or more dimensions. For this explanation, p is the dimension of a copula as well as the number of non-independent uniform random variables being considered for analysis.

In beginning the creation of a copula, we consider p uniform $U(0,1)$ random variables $U_1, ..., U_p$. Any continuous random variable can be transformed to be uniform over $(0,1)$ by its probability integral transformation. The relationship between these variables is described through their joint distribution function:

$$C(u_1, ..., u_p) = \text{Probability}(U_1 \geq u_1, ..., U_p \geq u_p) \tag{1}$$

Probability$(U_1 \geq u_1, ..., U_p \geq u_p)$ can relate to the marginal distributions of each variable. A marginal distribution is simply the cumulative distribution function of each of these individual variables. The cumulative distribution function (CDF) $F_X(x)$ describes the probability that a random variable X with a given probability distribution will be found at a value less than or equal to x.

Here C is the copula function. p-copula is the CDF of a multivariate distribution function with all of the univariate marginal distributions being uniform on the interval $[0,1]$.

Marginal distributions functions $F_1(x_1), ..., F_2(x_p)$ evaluated at $x_1, ..., x_p$ are then selected and C can be written as:

$$C(F_1(x_1), ..., F_p(x_p)) = C(u_1, ..., u_p) = F(x_1, ..., x_p) \tag{2}$$

which is a multivariate joint distribution function of all variables, evaluated at $x_1, ..., x_p$. That is done by transforming the univariate variables (x_n) into uniform variables (u_n) by applying a suitable marginal distribution (F_n). The dependence structure between variables is described by C. The variables input into the copula are the marginal distributions that represent each random variable.

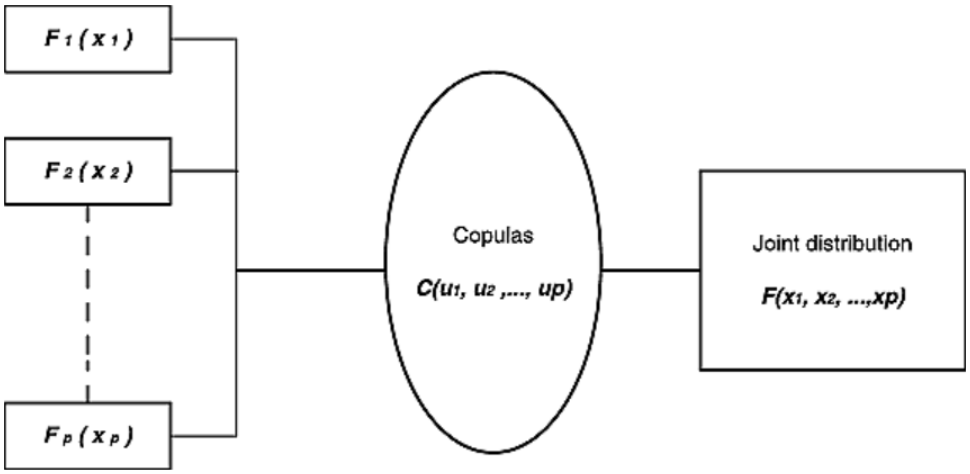

Figure 3.12: Representation of a copula. From Favre et al. (2004).

If the n-dimensional random sample (X_1, X_2, ..., X_n) is considered then the associated marginal distributions are $F_1(X_1), F_2(X_2)..., F_n(X_n)$. According to Sklar's theorem, if (X,Y,Z) are the trivariate random variables with continuous marginal distributions $u_1 = F_x(x) = P(X <= x)$, $u_2 = F_y(y) = P(Y <= y)$, and $u_3 = F_z(z) = P(Z <= z)$, then it can be characterized uniquely by its associated dependence function called a Copula (C) which can be defined on the unit square, can be expressed as;

$$H_{(x,y,z)} = C[F_x(x), F_y(y), F_z(z)] = C(u_1, u_2, u_3) \tag{3}$$

where, C is any type of copula. $F_x(x)$, are CDF of the univariate variables X, Y, and Z. $H_{(x,y)}$ is the bivariate joint distributions which can be expressed in terms of its univariate marginal functions and the associated dependence function C.

There are a multitude of copulas. Generally speaking, copulas may be grouped into the Archimedean copulas, meta-elliptical copulas, and copulas with prescribed geometric support (e.g., copulas with quadratic or cubic sections). According to their exchangeable properties, copulas may also be classified as symmetric copulas and asymmetric copulas. The most popular class of copulas is the Archimedean copulas Liebscher (2008). The Archimedean

family of copulas, which are widely applied in hydrology because they can be easily generated and are capable of capturing a wide range of dependence structures are used as the type of copula in this study.

The cumulative distribution functions of both the trivariate and bivariate copulas are used within the creation of return periods discussed in Section 3.3.5.

Within this project all code related to copulas is carried out in R utilizing the "Copula" Library. The copulas selected to model CCWE include four Archimedean copulas: the Frank Copula, Gumbel Copula, Joe Copula, and Clayton Copula. The copula dependence parameter is estimated using the maximum pseudo log-likelihood estimation procedure. The best fitted trivariate copulas are selected using the Cramer-von Mises distance statistics where the approximation of p-values for the test statistics are obtained using the faster multiplier bootstrapping approach

The copula methodology has been found to be an effective tool for multivariate modeling of flood risks, as the models preserve the dependence of different flood characteristics. Studies have applied copulas to flood frequency analysis (Chen et al., 2010; Favre et al., 2004), and flood coincidence risk analysis (Chen et al., 2012). Bivariate copula studies have shown dependence between flow and peak volume (Favre et al., 2004), and rainfall intensity and duration (De Michele and Salvadori, 2003). Bivariate Archimedean copulas have been used to simulate pairs of flood peak-volume to determine synthetic flood hydrographs (De Michele et al., 2005). Trivariate Copula studies have previously been done for rainfall frequency analysis (Balistrocchi and Bacchi, 2011), flood frequency analysis (Escalante-Sandoval and Raynal-Villasenor, 1994; Escalante-Sandoval and Raynal-Villasenor, 2008), analysis of flood risks (Ganguli and Reddy, 2013), modeling dependence structure of flood properties (Ganguli and Reddy, 2013), joint distribution of flood peak, volume and duration for flood frequency analysis (Grimaldi and Serinaldi, 2006), and relation between univariate and bivariate return periods in terms of Archimedean copulas (Salvadori and De Michele, 2004).

3.3.3 Univariate Analysis: Fitting Marginal Distributions

The first steps in creation of a copula model includes the fitting of marginal distributions for each variable of analysis (Figure 3.11). To perform the fitting or marginals, estimation of parameters, and goodness-of-fit measurements the MATLAB program AllFitDist was used. The continuous distributions considered include Beta, Birnbaum-Saunders, Exponential, Extreme value, Gamma, Generalized extreme value, Generalized Pareto, Inverse Gaussian, Logistic, Log-logistic, Lognormal, Nakagami, Normal, Rayleigh, Rician, t location-scale, and Weibull. The parameters of the marginal distributions are estimated through a maximum likelihood algorithm that minimizes the distance between empirical probability values and their modeled counterparts. We share a common assumption with the literature that the underlying marginal distribution does not change over time (Salvadori et al., 2014).

More than one distribution may fit the data well making the selection of the best model difficult. To circumvent this difficulty, the best fitting distribution for each variable was selected based on having the smallest values for Negative of the log likelihood (LogL), Bayesian information criterion (BIC), Akaike Information Criterion (AIC), and AIC with a correction for finite sample sizes (AICc). The best marginal distribution is selected based on the BIC. The parameters of the marginal distributions are estimated through a maximum likelihood algorithm that minimized the distance between empirical probability values and their modeled counterparts. Q-Q plot also used to verify the acceptability of the distribution fit. Using a wide range of distributions is essential to minimize prior assumptions on the distribution of data by selecting the best fitted function. Any distribution holds some underlying assumptions but our flexible approach strives to identify those closest to that of the underlying empirical distribution of data (Sadegh et al., 2018).

3.3.4 Assessing Dependence

The next step involved in the copula modeling procedure is to assess the dependence between modelled variables (Figure 3.11). To measure dependence between the flood driver proxy variables different graphical and common statistical tools were utilized, these include Pearson (r), Kendall tau (τ), and Spearman rho (ρ) correlation coefficients.. As the Pearson coefficient only measures linear dependence making it incompatible with heavy-tailed distributions, Kendall and Spearman are more appropriate for expressing the dependence between variables, such as those in this study, given they are non-parametric and based upon ranks.

3.3.5 Return Period

Return periods are defined as the average time between two of the same events (Salvadori and De Michele, 2004) and they are typically used within the risk assessment and communication sphere. Copulas allow for the easy estimation and creation of joint return periods (Salvadori, 2004; Salvadori and De Michele, 2004; Gräler et al., 2013; Latif and Mustafa, 2020).

In creating return periods, T, we are interested in the probability that a variable or variables exceed predetermined threshold values. Another way to think of this is the expected period between occurrence of two events with the same values, in the case of CCWE, the same amount of precipitation, tide level, and stream discharge. The threshold values in this case are based upon the annual CCWE values defined in Section 3.3.1.

The univariate return period considers the probability of one variable (i.e., X) exceeds a threshold value (i.e., x), as given below,

$$\begin{aligned} T_{Univariate} &= \frac{\mu}{\text{total number of events per year}} \\ &= \frac{1}{P(X \geq x)} = \frac{1}{(1 - F(x))} = \frac{1}{1 - CDF(x))} \end{aligned} \tag{4}$$

where $\mu = 1$ for annual based return periods, $T_{Univariate}$ = return period in years, and $F(x)$

= univariate CDF of variable.

Return periods can also be created with more than one variable. Joint return periods can be estimated using the inclusive probability also known as "OR" and "AND" cases(Salvadori and De Michele, 2004; Zhang and Singh, 2007; Latif and Mustafa, 2020). The type that is most relevant to the analysis of CCWE are joint "AND" return periods, which describes the situation that all variables simultaneously meet or exceed a certain threshold value during an event (i.e., $X_1 \geq x_1$, AND $X_2 \geq x_2 ...$ AND $X_n \geq x_n$) (Latif and Mustafa, 2020). While the "OR" cases only consider situations were at least one variable meets or exceeds a certain threshold value. To create these joint return periods, the cumulative distribution function (CDF) of the best fitted bivariate and trivariate copulas are utilized,

$$\begin{aligned} T^{AND}_{X,Y,Z}(x,y,z) &= \frac{1}{P(X \geq x \text{ AND } Y \geq y \text{ AND } Z \geq z)} \\ &= \frac{1}{1 - F(x) - F(y) - F(z) + H(x,y) + H(x,y) + H(y,z) - H(x,y,z)} \\ &= \frac{1}{1 - F(x) - F(y) - F(z) + C(F(x),F(y)) + C(F(x),F(y)) + C(F(y),F(z)) - C(F(x),F(y),F(z))} \end{aligned} \tag{5}$$

where $H(x,y,z)$ = trivariate CDF and $C(F(x),F(y),F(z))$ = trivariate copula CDF.

3.3.6 Focus Groups

The focus group was held on February 26, 2020, when planners, emergency managers and elected officials attended a workshop at the Murphy Center on East Carolina University's campus. This workshop was held as part of a larger National Oceanic and Atmospheric Administration (NOAA) Coastal Ocean Climate Applications (COCA)/Sectoral Applications Research Program (SARP) project: "Preparing for, Responding to, and Mitigating Compound Coastal Water Hazards for Resilient Rural Communities". The focus group was conducted by the NOAA COCA/SARP research project team members. Focus group discussions were conducted through two sessions. The first session divided all participants into geographically based regions. All participants were given the opportunity to respond to four questions relevant to their region in this session. The second session had all participants

at tables according to their profession. Questions within this session were from one of two groups depending upon the table. At each table there was also a facilitator and a note taker (Figure 3.13). The facilitator's role included directing the questions, focusing the discussion, and managing the time. The note taker's role was to record results on a large poster sheet. These sheets were hung up on a wall in the room after each session concluded for further discussions and to allow the participants to add comments through the use of post it notes (Figure 3.14).

Figure 3.13: Photo of focus group table during workshop held February 26, 2020.

The focus group consisted of representatives of three of the Planning Councils for eastern North Carolina. These councils include the Mid-East Commission, Albemarle Commission, the Cape Fear Council of Governments, and county-level emergency managers. Forty-one people participated in the focus group. The day was split into three sessions. Session 1 was the opening and introductions where an overview of the day's goals was given, and all participants were asked to introduce themselves to the group.

The questions presented in session 2 focused on the varied risk of flooding in each geographic region, delving into the types of floods that participants found most surprising,

frequent, and severe. The goal was to determine the relative risk of flood hazards and if they have been changing over time. To conclude this session, questions were asked to determine opportunities and obstacles in cooperating across jurisdictional boundaries along with challenges in securing resources. This session was organized by geographic region to get a better sense of the scope of flood types regionally, their relative importance, any changes they have noticed, and obstacles to addressing flood risk.

Session 3 focused on roles and responsibilities before, during, and after a flood event. The goal was to collect perspectives on the economic and health impacts witnessed, the technology and information sources people used or wish they had access to, the mitigation projects they have sought, along with the barriers to adequate preparation, response, recovery, and mitigation. This session was grouped by similar occupation or responsibility to know what their roles are regarding flood hazard management and corresponding perspectives on economic disruption and health impacts.

After concluding the focus group, the recordings were transcribed, and the poster notes were transcribed into a spreadsheet document. Pre-workshop survey data was reformatted into a spreadsheet and used to quantify perceptions based on the differing types of flooding (i.e., pluvial, fluvial, and ocean). The data analysis portion was performed in three steps by the qualitative team (Mukherji et al., 2021a). The first step was pre-analysis, where the focus group recordings were manually transcribed into text documents. Next was the first cycle of coding, descriptive coding (Saldana, 2009), which summarizes in a word or short phrase the basic topic of a passage. Last was the second cycle of coding, pattern coding (Miles and Huberman, 1994), which helps to identify emergent themes or explanations and is a good way of grouping summaries into sets or themes. The result of the second cycle of coding is used in this analysis.

Figure 3.14: Photo of poster hung on wall during workshop held February 26, 2020.

4 RESULTS

This section presents the primary results of the study for all areas of interest. The results are presented following the steps of fitting marginal distributions, creation of trivariate copulas, and construction of return period values. Finally, this section will conclude with a discussion of data collection within the focus group.

4.1 Marginal Distribution

The first step of the copula modelling approach is to find the distribution that best represents the data. Elaborated upon below is the best fit marginal distributions for all parameters in all study areas. Distributions that possess the minimum values of Negative of the log likelihood (NLogL), Bayesian information criterion (BIC, Schwarz, 1978), Akaike information criterion (AIC, Akaike (1973)), and AIC with a correction for finite sample sizes (AICc, Hurvich and Tsai, 1989) in comparison to the other candidates are selected to represent that variable. The NLogL is utilized in creating the following goodness of fit measures. Information theoretic criteria play an important role in model selection and most practitioners use AIC and BIC (Rao et al. 2010). The AIC is a method for scoring and selecting a model, it is optimal in the sense of minimizing the mean square error of predictions. AIC is defined in terms NLogL adjusted for the number of adjustable parameters in the model. The AIC statistic penalizes complex models less than BIC. BIC is also a method for scoring and selecting a model, this quantity is different, though proportional to AIC. BIC will tend to select the 'true' model as the size of the dataset increases. AICc, a corrected version of AIC, provides a stronger penalty or adjustment than AIC and BIC for small sample sizes. This measure is reported to have better small-sample behavior and will be used as the primary measure for this study (Brewer et al., 2016).

Within each of the following sections are tables listing the performance level of different univariate distributions for fitting the marginal distribution for the flood driver proxies,

parameters of these best fitting marginal distributions, and graphical goodness of fit visualizations. It is important to note that these are visual representations, and it cannot be associated with a degree of confidence. The graphics include, plotted empirical and theoretical densities, quantile-quantile (Q-Q) plot, the cumulative distribution functions (CDF), and corresponding probability-probability (P-P) plot for each proxy variable. Q-Q plots is a graphical technique for determining if two data sets come from populations with a common distribution, it plots the quantiles of the first data set against the quantiles of the second data set. If graph follows a linear pattern, it indicates that the distribution fits the given data well (Ramachandran and Tsokos, 2020). Q-Q plots take sample data, sorts it in ascending order, and then plot them versus quantiles calculated from a theoretical distribution. Similar to Q-Q plots, the P-P plot is a graphical tool to test how well a data set fits a distribution. This plot compares the empirical cumulative distribution functions of the given data with that of the assumed true cumulative probability distribution functions. If the plot of these two distributions is approximately linear, it indicates that the assumed true pdf gives a reasonably good fit to the given data that we seek to find its true distribution (Ramachandran and Tsokos, 2020).

4.1.1 Northern Case Study

Within the northern case study, the CCWE proxy drivers of precipitation, tide level, and stream discharge follow the Inverse Gaussian, Generalized Extreme Value, and Gamma distributions, whose parameters are within Table 4.1. Within the copula approach, it is not necessary to have the same distributions represent all variables. The best-fitted distributions to represent each driver were selected using AIC, BIC, and AICc, which are reported in Appendix D. The value with the smallest AIC is selected as the representative distribution. To confirm the selection of the marginal distributions, the empirical and theoretical densities (PDF), the quantile-quantile plots, the empirical and theoretical cumulative distribution function (CDF), and the probability-probability (P-P) plot, were plotted to the fitted dis-

tributions. It is important to note that the selected precipitation distribution (i.e., Inverse Gaussian) does not contain the smallest AIC. The Inverse Gaussian distributing has the second smallest AIC value of 349.47, though it does have the smallest BIC value of 352.53. The smallest AIC value of 349.47 belongs to the distribution Generalized Extreme Value. The decision to use Inverse Gaussian was made analyzing the graphical goodness-of-fit tests which are equally as important especially with relatively close values of AIC and BIC.

Using the estimated parameters for each distribution, we can obtain the comparison of the theoretical and empirical probabilities of the observed drivers. The distributions of CCWE proxy drivers are shown in the empirical and theoretical density plot (Figures 4.1a, 4.2a, and 4.3a). From the histogram, the distribution of stream discharge is highly right skewed. While the distributions of precipitation and tide level are skewed right though not as distinct. In these figures, the density of each best-fit distribution (i.e., the red line in each figure) fits the empirical histograms of each flood proxy driver. The Q-Q plots shows that the best-fit distributions and observed data sets come from roughly the same distribution (Figures 4.1b, 4.2b, and 4.3b). In a Q-Q plot, the values for the observed proxy variables (i.e., black circles) aligning in a straight line indicate the distribution is the exact same as the best-fit distribution. The Q-Q plot for tide level (Figure 4.2b) displays as relatively straight. While the Q-Q plots for precipitation and tide level curve off at the higher values indicating there are more extreme values than the best-fit distribution. In Figures 4.1c, 4.2c, and 4.3c, it is determined that the theoretical CDF of the best-fit distributions (i.e., red line) fit the empirical CDF for each respective flood proxy driver (i.e., black circles). Figures 4.1d, 4.2d, and 4.3d display the CDFs of the empirical and theoretical distributions against each other. Similar to the Q-Q plot, a straight line between the observed values (i.e., black circles) and best-fit distribution (i.e., black line) indicate the data sets are the same.

Table 4.1: Best Fit Marginal Distributions.

Variable	Distribution	Estimated Parameter(s)
Precipitation	Inverse Gaussian *(Figure 4.1)*	scale (μ) = 99.84 shape (λ) = 484.3533
Tide Level	Generalized Extreme Value *(Figure 4.2)*	shape (k) = 0.173 scale (σ) = 0.172 location (μ) = 1.327
Stream Discharge	Gamma *(Figure 4.3)*	shape (a) = 0.297 scale (b) = 186.252

Visual representation of goodness-of-fit in referenced figures.

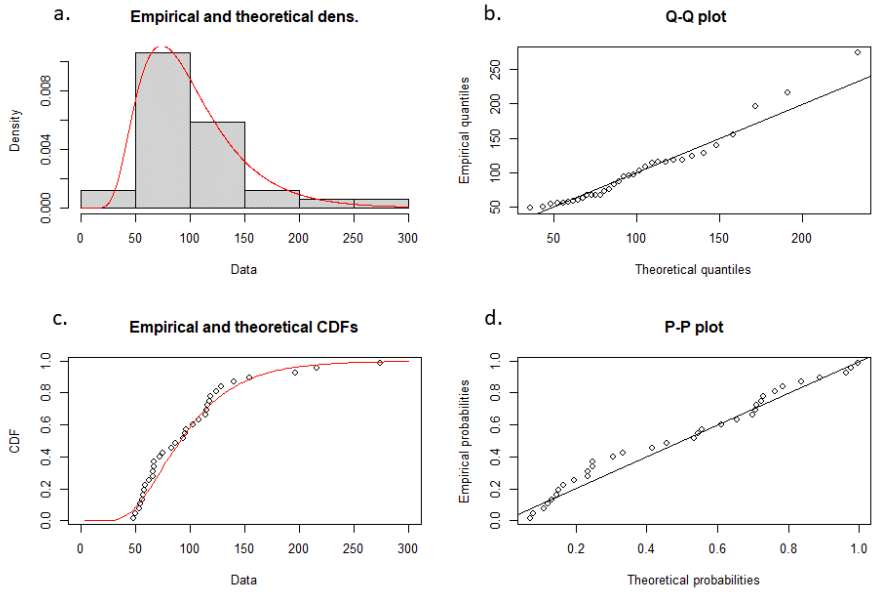

Figure 4.1: Inverse gaussian distribution visual goodness-of-fit measures for precipitation in the northern case study.

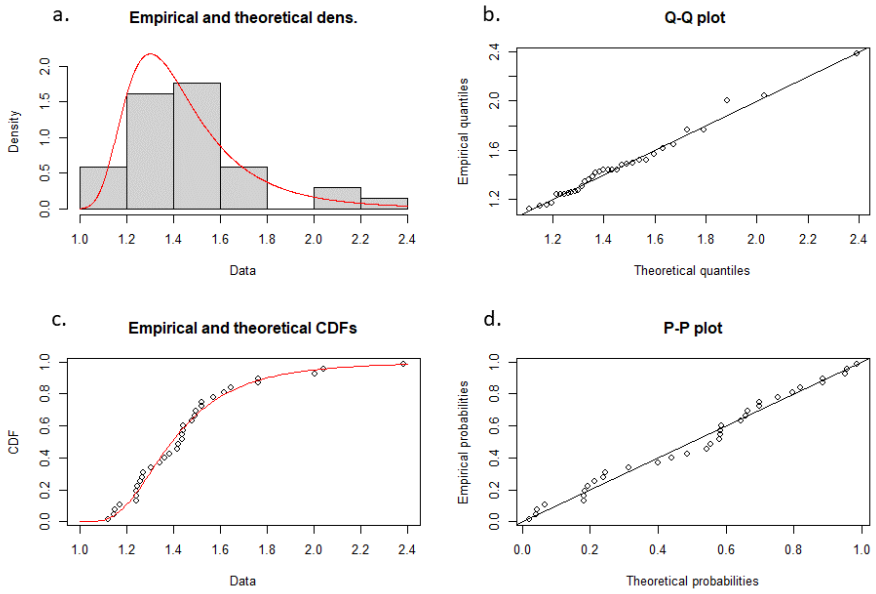

Figure 4.2: Generalized extreme value distribution visual goodness-of-fit measures for tide level in the northern case study.

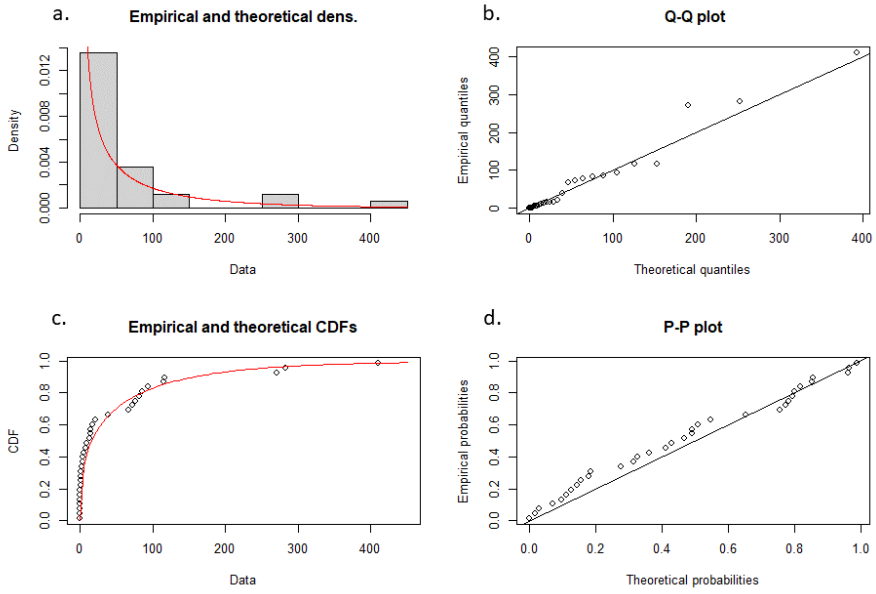

Figure 4.3: Gamma distribution visual goodness-of-fit measures for stream discharge in the northern case study.

4.1.2 Central Case Study

Within the CCWE case study, the CCWE proxy drivers of precipitation, tide level, and stream discharge follow the Inverse Gaussian, Generalized Extreme Value, and Weibull distributions, whose parameters are within Table 4.2. Note that within the copula approach, it is not necessary to have the same distributions represent all variables. The best-fitted distributions to represent each driver were selected using AIC, BIC, and AICc, which are reported in Appendix D. The value with the smallest AIC is selected as the representative distribution. To confirm the selection of the marginal distributions, the empirical and theoretical densities (PDF), the quantile-quantile plots, the empirical and theoretical cumulative distribution function (CDF), and the probability-probability (P-P) plot, were plotted to the fitted distributions.

Using the estimated parameters for each distribution, we can obtain the comparison of the theoretical and empirical probabilities of the observed drivers. The distributions of CCWE proxy drivers are shown in the empirical and theoretical density plot (Figures 4.4a, 4.5a, and 4.6a). From the histogram, the distribution of stream discharge is highly right skewed. While the distributions of precipitation and tide level are skewed right though not as distinct. In these figures, the density of each best-fit distribution (i.e., the red line in each figure) fits the empirical histograms of each flood proxy driver. The Q-Q plots shows that the best-fit distributions and observed data sets come from roughly the same distribution (Figures 4.4b, 4.5b, and 4.6b). In a Q-Q plot, the values for the observed proxy variables (i.e., black circles) aligning in a straight line indicate the distribution is the exact same as the best-fit distribution. The Q-Q plot for tide level (Figure 4.5b) displays as relatively straight. In Figures 4.4c, 4.5c, and 4.6c, it is determined that the theoretical CDF of the best-fit distributions (i.e., red line) fit the empirical CDF for each respective flood proxy driver (i.e., black circles). Figures 4.4d, 4.5d, and 4.6d display the CDFs of the empirical and theoretical distributions against each other. Similar to the Q-Q plot, a straight line between the observed values (i.e., black circles) and best-fit distribution (i.e., black line)

indicate the data sets are the same.

Table 4.2: Best Fit Marginal Distributions.

Variable	Distribution	Estimated Parameters
Precipitation	Inverse Gaussian *(Figure 4.4)*	Scale (μ) = 103.034 Shape (λ) = 484.354
Tide Level	Generalized Extreme Value *(Figure 4.5)*	Shape (k) = 0.191 Scale (σ) = 0.1671 Threshold (μ) = 1.214
Stream Discharge	Weibull *(Figure 4.6)*	Scale (A) = 35.499 Shape (B) = 0.691

Visual representation of goodness-of-fit in referenced figures.

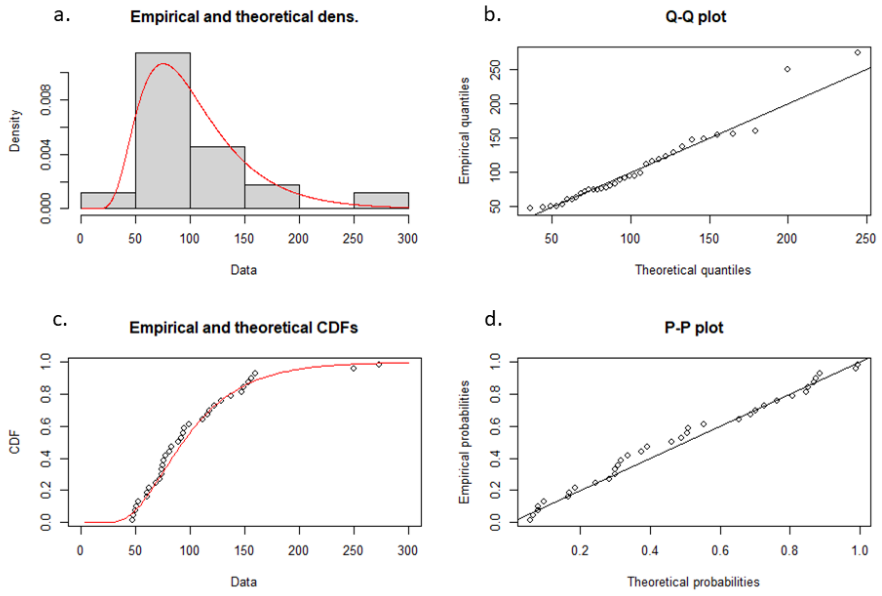

Figure 4.4: Inverse gaussian distribution visual goodness-of-fit measures for precipitation in the central case study.

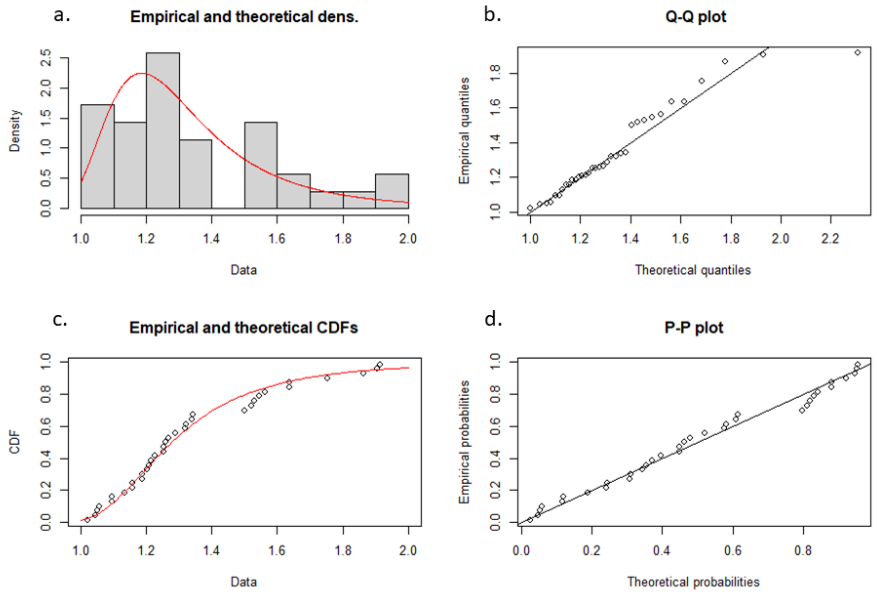

Figure 4.5: Generalized extreme value distribution visual goodness-of-fit measures for tide level in the central case study.

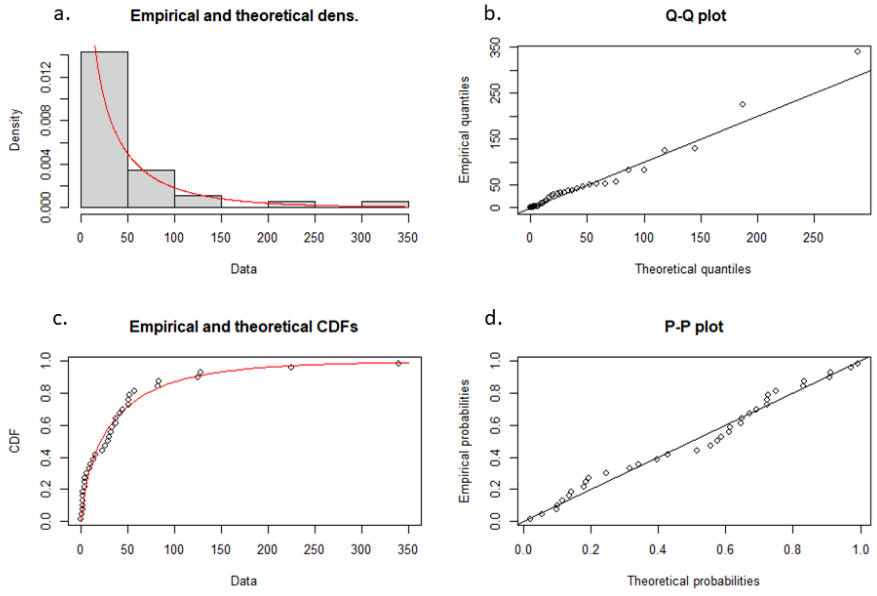

Figure 4.6: Weibull distribution visual goodness-of-fit measures for stream discharge in the central case study.

4.1.3 Southern Case Study

Within the southern case study, the CCWE proxy drivers of precipitation, tide level, and stream discharge follow the LogLogistic, Inverse Gaussian, and Birnbaum Saunders, whose parameters are within Table 4.3. Note that within the copula approach, it is not necessary to have the same distributions represent all variables. The best-fitted distributions to represent each driver were selected using AIC, BIC, and AICc, which are reported in Appendix D. The value with the smallest AIC is selected as the representative distribution. To confirm the selection of the marginal distributions, the empirical and theoretical densities (PDF), the quantile-quantile plots, the empirical and theoretical cumulative distribution function (CDF), and the probability-probability (P-P) plot, were plotted to the fitted distributions.

Using the estimated parameters for each distribution, we can obtain the comparison of the theoretical and empirical probabilities of the observed drivers. The distributions of CCWE proxy drivers are shown in the empirical and theoretical density plot (Figures 4.7a, 4.8a, and 4.9a). From the histogram, the distribution of stream discharge is highly right-skewed. While the the precipitation distribution is skewed right though not as distinct. Lastly, the tide level distribution exhibits minimal skewness. In these figures, the density of each best-fit distribution (i.e., the red line in each figure) fits the empirical histograms of each flood proxy driver. The Q-Q plots shows that the best-fit distributions and observed data sets come from roughly the same distribution (Figures 4.7b, 4.8b, and 4.9b). In a Q-Q plot, the values for the observed proxy variables (i.e., black circles) aligning in a straight line indicate the distribution is the exact same as the best-fit distribution. The Q-Q plot for tide level (Figure 4.8b) displays as relatively straight. In Figures 4.7c, 4.8c, and 4.9c, it is determined that the theoretical CDF of the best-fit distributions (i.e., red line) fit the empirical CDF for each respective flood proxy driver (i.e., black circles). Figures 4.7d, 4.8d, and 4.9d display the CDFs of the empirical and theoretical distributions against each other. Similar to the Q-Q plot, a straight line between the observed values (i.e., black circles) and best-fit distribution (i.e., black line) indicate the data sets are the same.

Table 4.3: Best Fit Marginal Distributions.

Variable	Distribution	Estimated Parameters
Precipitation	LogLogistic *(Figure 4.7)*	Log Location (μ) = 5.718431; Log Scale (σ) = 90.2906
Tide Level	Inverse Gaussian *(Figure 4.8)*	Scale (μ) = 1.643; Shape (λ) = 77.345
Stream Discharge	Birnbaum Saunders *(Figure 4.9)*	Scale (β) = 161.79; Shape = (γ) = 1.203

Visual representation of goodness-of-fit in referenced figures

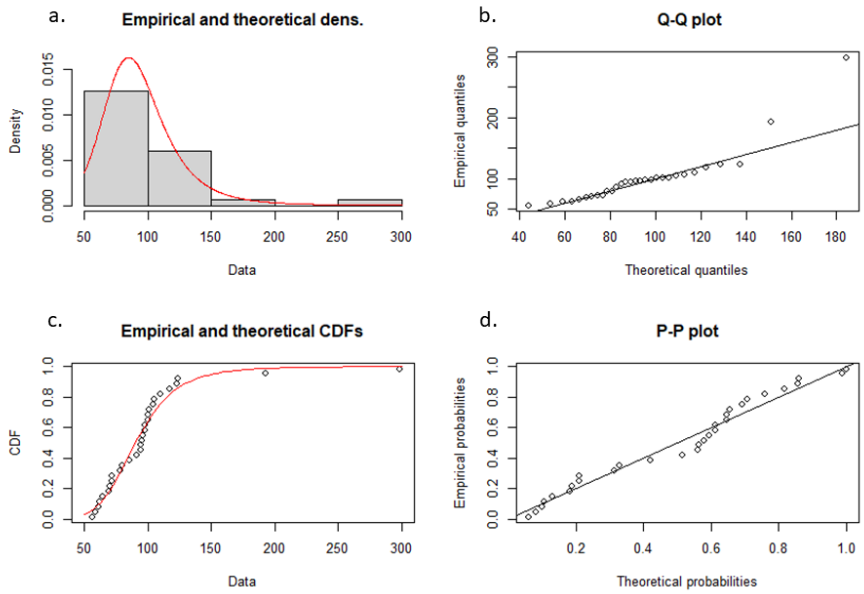

Figure 4.7: LogLogistic distribution visual goodness-of-fit measures for precipitation in the southern case study.

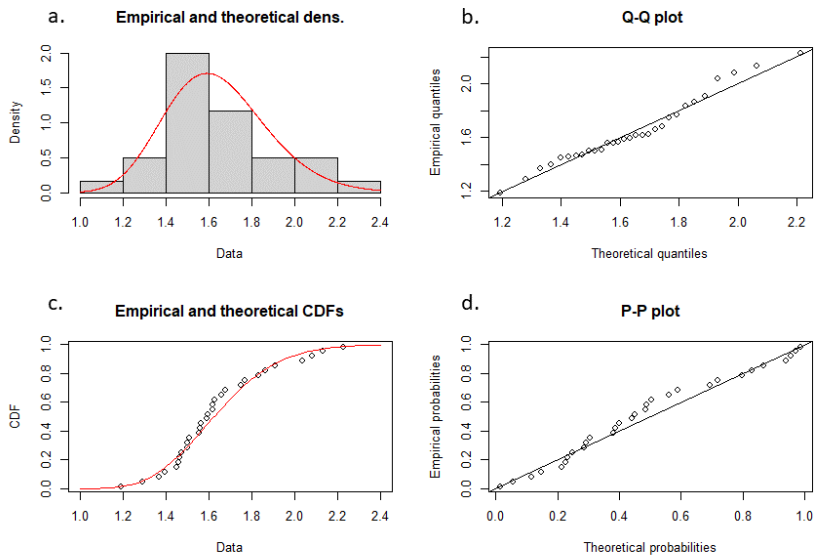

Figure 4.8: Inverse Gaussian distribution visual goodness-of-fit measures for tide level in the southern case study.

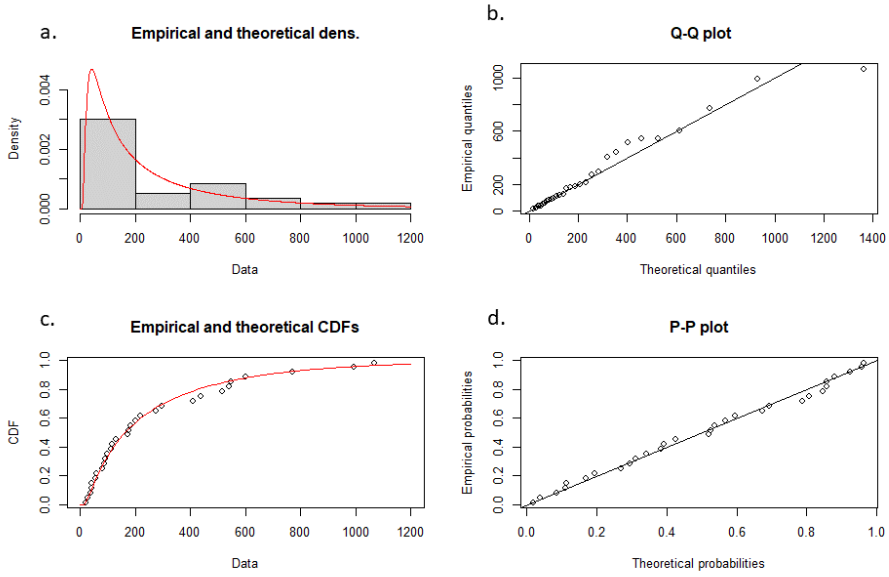

Figure 4.9: Birnbaum Saunders distribution visual goodness-of-fit measures for stream discharge in the southern case study.

4.2 Correlations

After marginal distribution functions were defined, dependence between separate variables was assessed. The strength of dependency between the flood drivers' proxies i.e., precipitation, stream discharge, and tide level are estimated using Pearson's linear correlation (r), and the two non-parametric dependence measures, also called the rank based correlations statistics such as Kendall's tau (τ) and Spearman's rho (ρ). These values are located in Tables 4.4, 4.5, 4.6. All dependencies except Pearson's tide - stream are statistically significant. The strongest dependence within all the study areas is between precipitation and tide level, with the second strongest dependence between precipitation and stream discharge.

Table 4.4: Northern Study Area: Station variable-pair correlations

Variable Pair	Pearson r	Spearman ρ	Kendall τ
Precipitation - Tide Level	0.433 (0.011)*	0.466 (0.006)*	0.307 (0.011)*
Precipitation - Stream Discharge	0.418 (0.014)*	0.466 (0.006)*	0.366 (0.002)*
Tide Level - Stream Discharge	0.140 (0.429)	0.419 (0.014)*	0.293 (0.015)*

Table 4.5: Central Study Area: Station variable-pair correlations

Variable Pair	Pearson r	Spearman ρ	Kendall τ
Precipitation - Tide Level	0.644 (0)*	0.578 (0)*	0.409 (0)*
Precipitation - Stream Discharge	0.755 (0)*	0.470 (0.004)*	0.343 (0.004)*
Tide Level - Stream Discharge	0.4 (0.017)*	0.345 (0.042)*	0.259 (0.029)*

Table 4.6: Southern Study Area: Station variable-pair correlations

Variable Pair	Pearson r	Spearman ρ	Kendall τ
Precipitation - Tide Level	0.689 (0)*	0.579 (0)*	0.411 (0.002)*
Precipitation - Stream Discharge	0.675 (0)*	0.379 (0.039)*	0.263 (0.042)*
Tide Level - Stream Discharge	0.689 (0)*	0.421 (0.021)*	0.255 (0.048)*

4.3 Trivariate Copulas

In this study a total of four Archimedean families that capture different kinds of joint dependence structures are used: Clayton, Gumbel, Frank, and Joe. The Clayton, Gumbel and

Joe copulas describe an asymmetrical tail behavior, while the Frank copula captures joint symmetric dependence. While Gumbel and Joe copulas can represent upper tail dependence, Clayton copulas can represent lower tail dependence. They are tested for their goodness-of-fit for modelling trivariate CCWE hazard proxies. The copulas dependence parameters are estimated using maximum pseudo log-likelihood (or MPL) estimation procedure. Identification and selection of best-fit copulas for establishing the trivariate joint distribution is performed using the Cramér–von Mises distance statistics (S_n) with parametric bootstrap procedure. The Cramér–von Mises criterion is a criterion used for judging the goodness of fit of two distributions. According to Genest et al. (2009), Cramér–von Mises test is the most powerful goodness of fit test based on empirical process. P-values for Cramér–von Mises test can be calculated with the parametric bootstrap procedure (Bezak et al., 2014). This statistic has been computed from 1000 simulated random sample by the mean of faster, multiplier approach and the estimated values are in Tables 4.7, 4.9, 4.10.

4.3.1 Northern Case Study

Within the northern case study based upon S_n, the best fit copula for the trivariate model was the Frank copula, see Appendix C for the equation. The estimated copula parameters and goodness-of-fit measures are presented in table 4.7.

First, within the northern case study the best fit copula for the trivariate model was the Frank Copula. This copula maintained consistency in the dependency structure of CCWE between the observed and modelled points as shown in Section 4.4.1.

Table 4.7: Three-dimensional copula goodness-of-fit measures and copula parameters.

Copula Family	Parameter Estimates	Maximized Log Likelihood	Sn
Gumbel	1.503	9.896	0.042
Clayton	0.735	7.868	—
Frank	3.475	10.95	**0.037**
Joe	1.712	8.374	0.0672

Figures 4.10 and 4.10 represent the simulations on 2-dimensional and 3-dimensional scatter plots. Through these scatter plots it can be observed that the frank copula produced events that adequately overlap with the dependence pattern of observed CCWE.

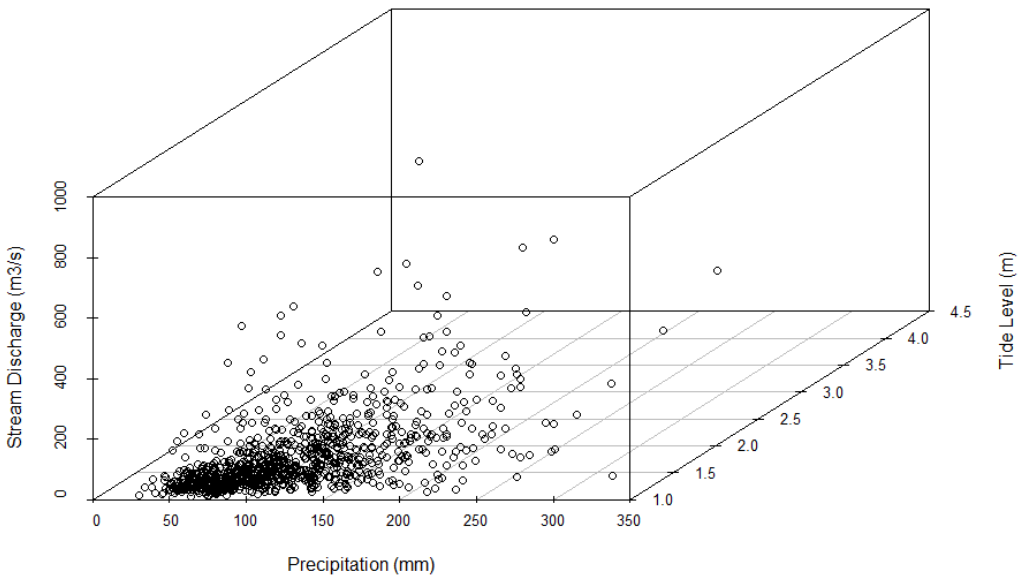

Figure 4.10: Scatterplot of simulated CCWE events created from the 3-dimensional frank copula within the northern case study.

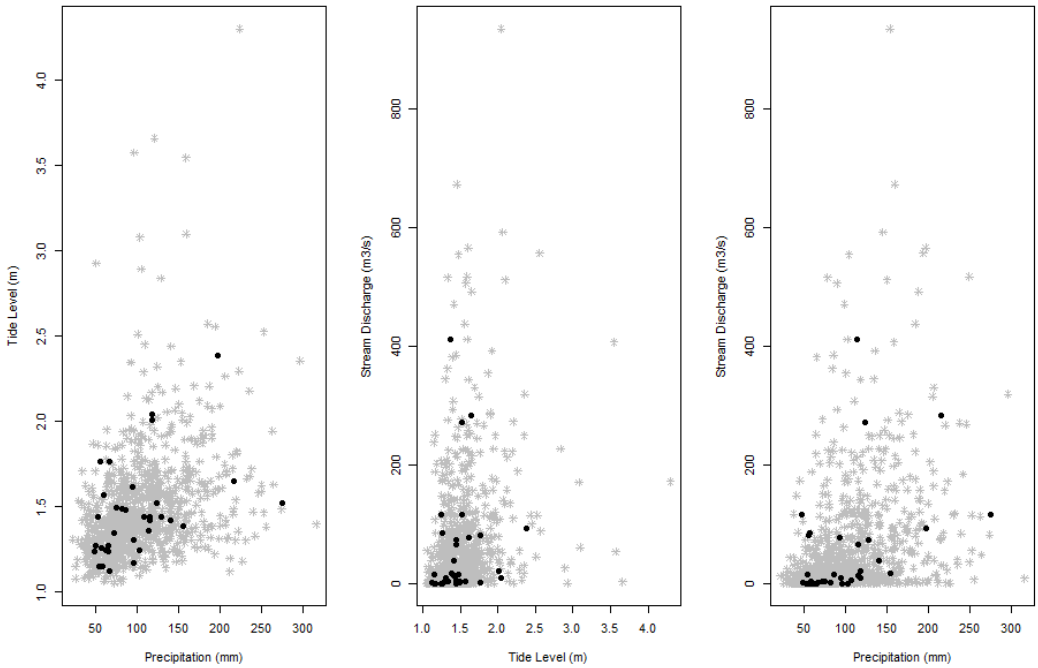

Figure 4.11: Scatterplot of simulated CCWE events created from the 3-dimensional frank copula (grey asterisks) and actual CCWE events (black circles) within the northern case study.

4.3.2 Central Case Study

In the central case study, based upon S_n, the best fit copula for the trivariate model was the Gumbel copula, see Appendix C for the equation. The estimated copula parameters and goodness-of-fit measures are presented in 4.9.

Table 4.8: Three-dimensional copula goodness-of-fit measures and copula parameters.

Copula Family	Parameter Estimates	Maximized Log Likelihood	Sn
Gumbel	1.559	14.05	**0.040**
Clayton	0.723	7.298	—
Frank	3.195	10.60	0.069
Joe	1.895	14.57	0.042

Table 4.9: Three-dimensional copula goodness-of-fit measures and copula parameters.

Copula Family	Parameter Estimates	Maximized Log Likelihood	Sn
Gumbel	1.559	14.05	**0.040**
Clayton	0.723	7.298	—
Frank	3.195	10.60	0.069
Joe	1.895	14.57	0.042

Figures 4.12 and 4.13 represent the simulations on 2-dimensional and 3-dimensional scatter plots. Through these scatter plots it can be observed that the frank copula produced events that adequately overlap with the dependence pattern of observed CCWE.

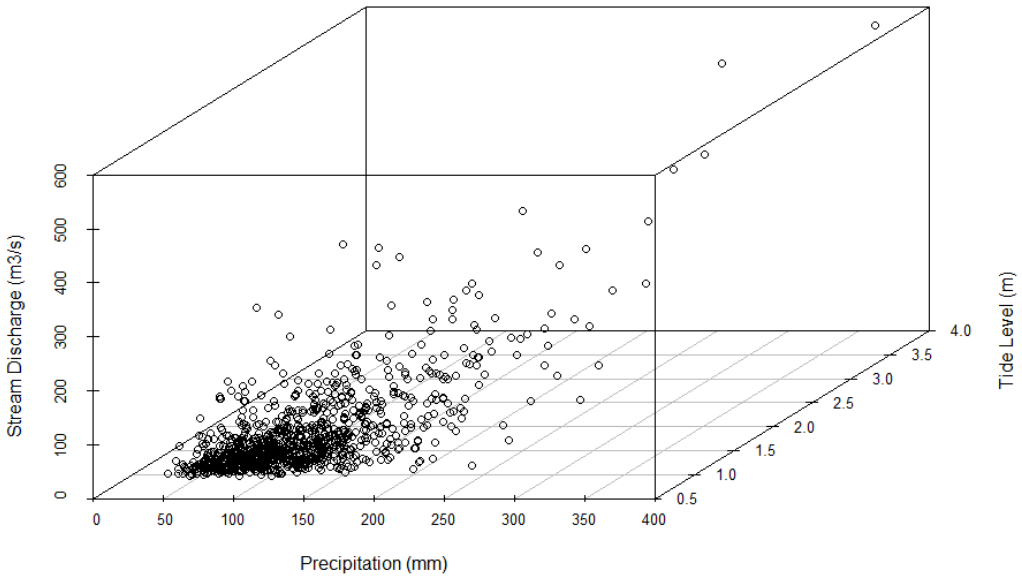

Figure 4.12: Scatterplot of simulated CCWE events created from the 3-dimensional frank copula within the central case study.

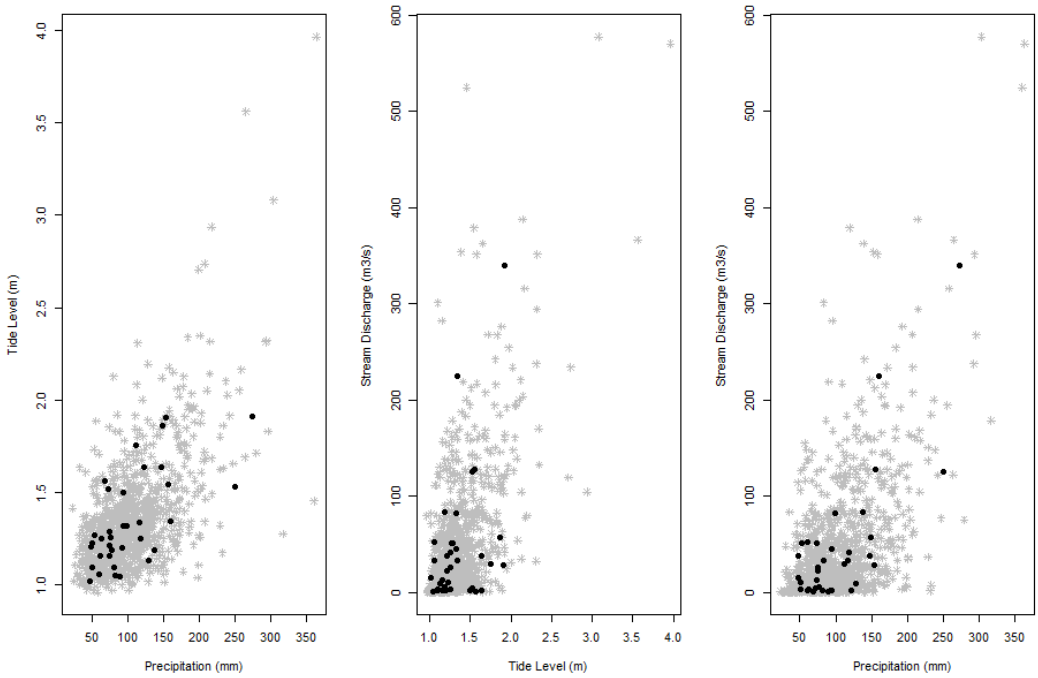

Figure 4.13: Scatterplot of simulated CCWE events created from the 3-dimensional frank copula (grey asterisks) and actual CCWE events (black circles) within the central case study.

4.3.3 Southern Case Study

Within the southern case study, based upon S_n, the best fit copula for the trivariate model was the Joe copula, see Appendix C for the equation. The estimated copula parameters and goodness-of-fit measures are presented in 4.10.

Table 4.10: Three-dimensional copula goodness-of-fit measures and copula parameters.

Copula Family	Parameter Estimates	Maximized Log Likelihood	Sn
Gumbel	1.699	15.63	0.071
Clayton	0.805	7.121	—
Frank	3.439	9.992	0.109
Joe	2.2	17.28	**0.049**

Figures 4.14 and 4.15 represent the simulations on 2-dimensional and 3-dimensional scatter plots. Through these scatter plots it can be observed that the frank copula produced events that adequately overlap with the dependence pattern of observed CCWE.

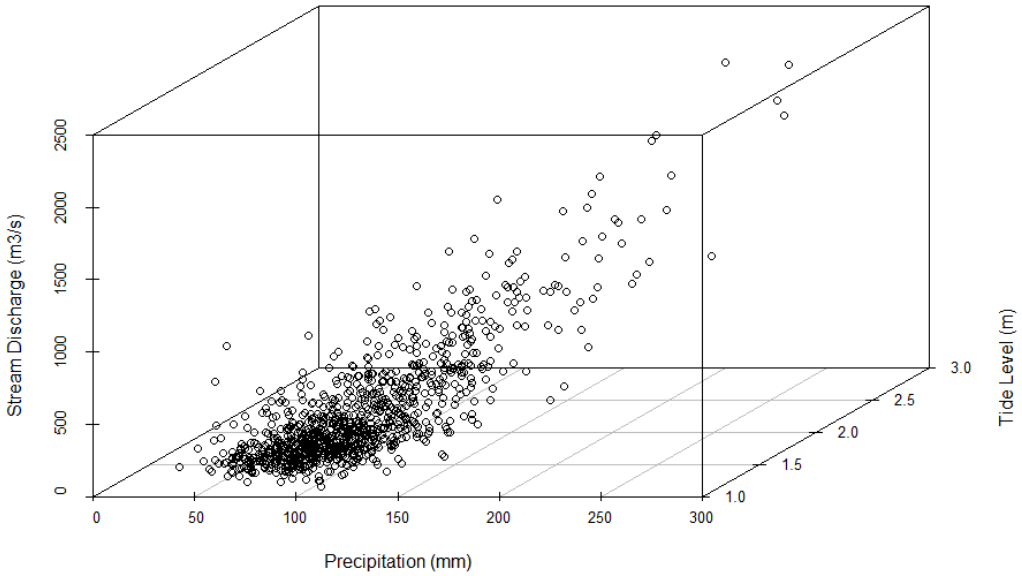

Figure 4.14: Scatterplot of simulated CCWE events created from the 3-dimensional Frank Copula within the southern case study.

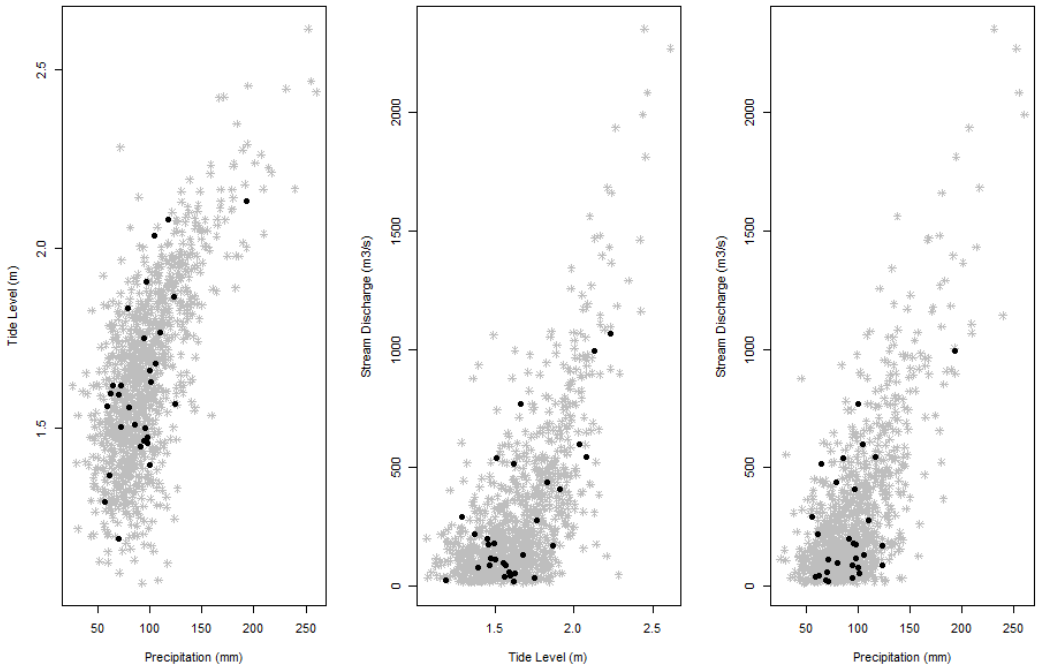

Figure 4.15: Scatterplot of simulated CCWE events created from the 3-dimensional Frank Copula (grey asterisks) and actual CCWE events (black circles) within the southern case study.

4.4 Return Period

4.4.1 Univariate

The univariate return periods are derived from the best-fitted CDFs for each flood characteristic. Tables 4.14, 4.15, and 4.16 present the return period (T) for each observed CCWE and corresponding values of precipitation, tide level, and stream discharge. It is important to note that estimation and use of univariate return periods could cause underestimation or overestimation of risk in CCWE, considering all drivers and creating a trivariate return period will be discussed in the next section.

Table 4.11: Univariate return period (T; years) derived from best-fit distributions for CCWE flood drivers in the northern case study.

CCWE Event ($Year$)	Precip. (mm)	Tide (m)	Stream (m^3/s)	T(Precip)	T(Tide)	T(Stream)
1987	66	1.268	0.040	1.307	1.315	1.074
1988	67.3	1.122	0.680	1.331	1.022	1.218
1989	96.5	1.171	0.164	2.254	1.072	1.125
1990	49.5	1.271	0.765	1.088	1.326	1.228
1991	108	1.439	5.635	2.889	2.396	1.565
1992	57.2	1.256	84.951	1.170	1.273	5.032
1993	54.6	1.149	14.725	1.139	1.045	1.967
1994	115.6	1.442	66.261	3.431	2.425	4.098
1995	95.3	1.302	9.599	2.199	1.455	1.752
1996	140	1.417	38.228	6.148	2.198	2.889
1997	53.3	1.438	0.003	1.125	2.387	1.030
1998	55.9	1.762	81.269	1.154	8.675	4.838
1999	114.3	1.362	410.594	3.330	1.786	78.199
2000	115.8	1.422	12.658	3.447	2.241	1.882
2001	86.4	1.479	14.640	1.841	2.811	1.963
2002	66	1.24	0.001	1.307	1.222	1.017
2003	196.9	2.383	93.446	26.320	66.367	5.499
2004	48.3	1.24	116.382	1.078	1.222	6.914
2005	154.9	1.385	16.452	8.916	1.945	2.036
2006	128.5	1.44	72.774	4.648	2.406	4.410
2007	62.2	1.246	0.000	1.242	1.240	1.000
2008	57.7	1.147	0.105	1.177	1.043	1.106
2009	118.6	2.006	20.841	3.678	20.835	2.209
2010	124.2	1.521	270.709	4.195	3.332	26.409
2011	274.6	1.52	114.966	205.441	3.318	6.820
2012	82.6	1.49	0.450	1.715	2.939	1.184
2013	67.3	1.761	0.351	1.331	8.642	1.167
2014	74.9	1.494	4.106	1.498	2.987	1.482
2015	102.6	1.242	0.236	2.566	1.228	1.143
2016	215.9	1.647	282.319	43.353	5.540	28.986
2017	59.2	1.569	2.512	1.197	4.048	1.382
2018	72.4	1.342	3.710	1.439	1.663	1.459
2019	118.1	2.044	8.353	3.635	23.656	1.696
2020	94	1.616	76.739	2.141	4.894	4.607

Table 4.12: Univariate return period (T; years) derived from best-fit distributions for CCWE flood drivers in the central case study.

CCWE Event ($Year$)	Precip. (mm)	Tide (m)	Stream (m^3/s)	T(Precip)	T(Tide)	T(Stream)
1980	60.7	1.056	51.820	1.199	1.063	3.665
1981	99.1	1.319	81.836	2.241	2.360	5.935
1982	82.6	1.050	32.564	1.648	1.055	2.566
1983	89.2	1.044	0.566	1.854	1.048	1.059
1984	118.1	1.252	41.343	3.336	1.818	3.038
1985	122.4	1.636	2.240	3.667	8.376	1.160
1986	116.1	1.340	33.131	3.194	2.568	2.595
1987	52.8	1.267	51.253	1.109	1.924	3.629
1988	62.7	1.252	3.568	1.228	1.818	1.227
1989	61.0	1.157	1.331	1.203	1.319	1.109
1990	75.4	1.258	26.250	1.465	1.860	2.252
1991	74.7	1.215	22.200	1.449	1.590	2.061
1992	73.9	1.288	50.970	1.431	2.087	3.611
1993	50.5	1.096	3.398	1.088	1.135	1.219
1994	94.0	1.322	44.741	2.029	2.388	3.233
1995	50.3	1.227	10.081	1.086	1.659	1.521
1996	148.8	1.863	56.917	6.721	18.802	3.998
1997	47.0	1.021	15.263	1.062	1.026	1.748
1998	147.6	1.638	37.661	6.534	8.440	2.835
1999	273.6	1.915	339.802	146.335	22.315	116.793
2000	73.9	1.158	13.196	1.431	1.323	1.657
2001	92.2	1.203	2.322	1.960	1.525	1.164
2002	48.3	1.208	37.378	1.071	1.552	2.819
2003	137.9	1.186	82.968	5.211	1.442	6.036
2004	72.1	1.520	3.823	1.393	5.334	1.239
2005	156.0	1.546	127.992	7.972	5.913	11.306
2006	160.3	1.343	225.402	8.835	2.599	36.063
2007	68.6	1.562	0.141	1.325	6.298	1.022
2008	94.2	1.501	1.713	2.036	4.943	1.131
2009	111.5	1.755	29.733	2.893	12.960	2.423
2010	250.2	1.530	124.877	81.367	5.550	10.853
2011	153.7	1.905	28.600	7.547	21.600	2.367
2012	128.8	1.132	8.722	4.232	1.232	1.461
2013	80.8	1.094	1.388	1.599	1.131	1.112
2014	77.2	1.188	5.720	1.507	1.451	1.328

Table 4.13: Univariate return period (T; years) derived from best-fit distributions for CCWE flood drivers in the southern case study.

CCWE Event ($Year$)	Precip. (mm)	Tide (m)	Stream (m^3/s)	T(Precip)	T(Tide)	T(Stream)
1980	69.6	1.192	25.627	1.226	1.016	1.041
1981	123.7	1.566	85.800	7.051	1.664	1.420
1982	97.8	1.457	174.715	2.579	1.292	2.107
1983	105.4	1.679	129.408	3.423	2.431	1.743
1984	61.5	1.368	216.907	1.111	1.133	2.479
1985	59.2	1.56	41.343	1.089	1.637	1.124
1986	69.9	1.591	60.032	1.231	1.791	1.243
1987	71.6	1.502	113.267	1.265	1.416	1.620
1988	56.1	1.292	294.495	1.066	1.060	3.261
1989	85.3	1.509	540.852	1.722	1.438	6.974
1990	100.3	1.396	78.721	2.824	1.173	1.371
1991	97.8	1.472	116.665	2.579	1.329	1.646
1993	101.1	1.627	54.085	2.909	2.012	1.204
1996	193	2.132	993.921	78.018	32.692	23.660
1997	79.8	1.556	99.392	1.493	1.619	1.518
1998	100.3	1.661	770.218	2.824	2.270	13.164
1999	298.5	2.229	1067.545	933.372	68.588	28.558
2000	95.5	1.498	181.511	2.378	1.403	2.165
2005	91.2	1.449	199.067	2.059	1.273	2.318
2006	110.2	1.767	276.089	4.125	3.540	3.063
2007	71.6	1.619	20.247	1.265	1.959	1.020
2008	104.1	2.036	600.317	3.257	16.610	8.260
2009	96.5	1.909	407.763	2.463	7.468	4.695
2010	78.7	1.833	438.911	1.456	4.906	5.164
2011	62.2	1.597	42.192	1.119	1.825	1.129
2012	94.5	1.463	90.048	2.298	1.306	1.451
2013	64.8	1.617	515.367	1.150	1.946	6.478
2014	94.2	1.749	36.246	2.274	3.260	1.095
2015	117.3	2.082	546.515	5.466	22.808	7.089
2016	123.2	1.866	172.733	6.913	5.855	2.091

4.4.2 Trivariate

In the following tables 4.14, 4.15, 4.16, each row represents an annual CCWE defined in Section 3.3.1. The columns *Precip. (mm)*, *Tide (m)*, and *Stream (m^3/s)* are values from each CCWE. Both the "AND" and "OR" joint return periods are represented. The "AND" return period represents the probability that the *Precip. (mm)*, *Tide (m)*, and *Stream (m^3/s)* meet or exceed the values measured within that event. The "OR" return period represents the probability that at least one of the drivers, *Precip. (mm)*, *Tide (m)*,

or *Stream* (m^3/s), meet or exceed the values they measured in that event. The type that is most relevant to the analysis of CCWE are joint "AND" return periods as we are interested in all variables occurring at extreme levels at the same time. The probability of exceeding all measurements at the same time (T_{PTS}^{AND}) is less than the probability that at least one of the driver measurements is exceeded (T_{PTS}^{OR}). Hence, it is inferred that the occurrence of trivariate flood drivers simultaneously is less frequent in the "AND" case and more frequent in the "OR" case.

Through all of the modelled points return periods are able to be created for all of the observed CCWE and their in-situ driver measurements. The maximum observed measurements for all three drivers within the temporal extent of this analysis occur within different CCWE. The maximum precipitation occurs 8/27/2011 with a value of 274.6 $millimeters$ and a univariate return period of 205 years. The maximum tide level measurement of of 2.383 $meters$ occurs within a CCWE on 9/18/2003 and this value of tide level has a univariate return period of 66 years. The maximum corresponding stream discharge occurs 9/17/1999 with a value of 410.59 m^3/s and return period of 78 years. The maximum "AND"-based joint return period for all values occurs on 8/27/2011, the same date as maximum station precipitation, with a return period of 400 years. The next largest "AND"-based return period occurs with Hurricane Floyd with variable values of precipitation of 114.3 $millimeters$, tide level of 1.362 $meters$, stream discharge of 410.594 m^3/s, and a return period of 155 years.

Table 4.14: Trivariate return period (years) for CCWE flood drivers in the northern case study.

CCWE Event ($Year$)	Precip. (mm)	Tide (m)	Stream (m^3/s)	T_{PTS}^{AND} (years)	T_{PTS}^{OR} (years)
1987	66	1.268	0.040	1.623	1.022
1988	67.3	1.122	0.680	1.533	1.006
1989	96.5	1.171	0.164	2.406	1.018
1990	49.5	1.271	0.765	1.579	1.022
1991	108	1.439	5.635	5.104	1.348
1992	57.2	1.256	84.951	5.588	1.072
1993	54.6	1.149	14.725	2.108	1.012
1994	115.6	1.442	66.261	8.939	1.799
1995	95.3	1.302	9.599	3.311	1.219
1996	140	1.417	38.228	10.902	1.723
1997	53.3	1.438	0.003	2.491	1.008
1998	55.9	1.762	81.269	20.269	1.143
1999	114.3	1.362	410.594	155.487	1.622
2000	115.8	1.422	12.658	5.985	1.467
2001	86.4	1.479	14.640	4.829	1.385
2002	66	1.24	0.001	1.501	1.005
2003	196.9	2.383	93.446	80.401	4.775
2004	48.3	1.24	116.382	7.399	1.033
2005	154.9	1.385	16.452	13.647	1.502
2006	128.5	1.44	72.774	10.930	1.892
2007	62.2	1.246	0.000	1.448	1.000
2008	57.7	1.147	0.105	1.299	1.005
2009	118.6	2.006	20.841	38.649	1.879
2010	124.2	1.521	270.709	48.229	2.430
2011	274.6	1.52	114.966	400.026	2.780
2012	82.6	1.49	0.450	3.855	1.118
2013	67.3	1.761	0.351	9.913	1.082
2014	74.9	1.494	4.106	4.044	1.204
2015	102.6	1.242	0.236	2.875	1.052
2016	215.9	1.647	282.319	106.289	4.754
2017	59.2	1.569	2.512	4.771	1.098
2018	72.4	1.342	3.710	2.426	1.140
2019	118.1	2.044	8.353	47.646	1.571
2020	94	1.616	76.739	12.794	1.797

Next, within the central NC case study the maximum measured values for the proxy variables occur within the same year ranging from the dates 9/16/1999 to 9/17/1999 which coincided with Hurricane Floyd. The maximum 24-hour precipitation was 273.6 $millimeters$, with a univariate return period of 146 years; the corresponding tide level measurement was 1.915 m with a univariate return period of 22.3 years; and the corresponding stream discharge

was 339.8 m^3/s with a univariate return period of 116 years. The "AND"-based joint return period for all of these values occurring at one was 215 years, which means all of these drivers are more common on their own than occurring at the same time.

Table 4.15: Trivariate return period (years) for CCWE flood drivers in the central case study.

CCWE Event ($Year$)	Precip. (mm)	Tide (m)	Stream (m^3/s)	T_{PTS}^{AND} (years)	T_{PTS}^{OR} (years)
1980	60.7	1.056	51.820	3.759	1.025
1981	99.1	1.319	81.836	6.726	1.642
1982	82.6	1.05	32.564	3.005	1.036
1983	89.2	1.044	0.566	1.923	1.008
1984	118.1	1.252	41.343	4.977	1.507
1985	122.4	1.636	2.240	10.270	1.144
1986	116.1	1.34	33.131	5.025	1.665
1987	52.8	1.267	51.253	4.754	1.078
1988	62.7	1.252	3.568	2.175	1.059
1989	61	1.157	1.331	1.562	1.024
1990	75.4	1.258	26.250	3.212	1.216
1991	74.7	1.215	22.200	2.789	1.169
1992	73.9	1.288	50.970	4.667	1.264
1993	50.5	1.096	3.398	1.406	1.014
1994	94	1.322	44.741	4.617	1.506
1995	50.3	1.227	10.081	2.233	1.041
1996	148.8	1.863	56.917	16.594	3.233
1997	47	1.021	15.263	1.811	1.005
1998	147.6	1.638	37.661	11.757	2.424
1999	273.6	1.915	339.802	215.075	20.725
2000	73.9	1.158	13.196	2.207	1.099
2001	92.2	1.203	2.322	2.445	1.077
2002	48.3	1.208	37.378	3.458	1.043
2003	137.9	1.186	82.968	8.446	1.388
2004	72.1	1.52	3.823	5.956	1.110
2005	156	1.546	127.992	15.319	4.049
2006	160.3	1.343	225.402	30.973	2.453
2007	68.6	1.562	0.141	6.605	1.013
2008	94.2	1.501	1.713	5.748	1.098
2009	111.5	1.755	29.733	11.198	1.873
2010	250.2	1.53	124.877	259.770	4.695
2011	153.7	1.905	28.600	20.713	2.221
2012	128.8	1.132	8.722	4.753	1.115
2013	80.8	1.094	1.388	1.766	1.023
2014	77.2	1.188	5.720	2.102	1.092

Lastly, in the southeastern case study location the maximum values of all proxy variables

are all within the same event which occurred 9/16/1999 to 9/19/1999. These dates also coincide with Hurricane Floyd. For this event the maximum in-situ precipitation value is 298.5 $millimeters$ which has a return period of 933 years. The coinciding in-situ tide level value of 2.229 $meters$ has a return period of 68 years, while the coinciding in-situ stream discharge value of 1067.5 m^3/s has a return period of 28 years. Within a CCWE all of these values are occurring simultaneously which can be represented by the joint "AND" return period. The return period of all these occurring or being exceeded has a value of 833 years. This suggests that precipitation accompanied by these extreme values of stream discharge and tide level are more likely to occur than extreme precipitation on its own. The values that represent closest to a 100-year return period (actually 109 years) are 193 $millimeters$ precipitation, 2.132 m tide level, and 993.9 m^3/s stream discharge. The values that represent a 50-year return period are 117 $millimeters$ precipitation, 2.082 $meters$ tide level, and 546.5 m^3/s stream discharge.

Table 4.16: Trivariate return period (years) for CCWE flood drivers in the southern case study.

CCWE Event ($Year$)	Precip. (mm)	Tide (m)	Stream (m^3/s)	T_{PTS}^{AND} (years)	T_{PTS}^{OR} (years)
1980	69.6	1.192	25.627	1.271	1.000
1981	123.7	1.566	85.800	7.441	1.223
1982	97.8	1.457	174.715	3.654	1.179
1983	105.4	1.679	129.408	4.563	1.460
1984	61.5	1.368	216.907	2.633	1.020
1985	59.2	1.56	41.343	1.779	1.012
1986	69.9	1.591	60.032	2.079	1.050
1987	71.6	1.502	113.267	2.100	1.072
1988	56.1	1.292	294.495	3.338	1.007
1989	85.3	1.509	540.852	7.131	1.242
1990	100.3	1.396	78.721	3.194	1.067
1991	97.8	1.472	116.665	3.231	1.155
1993	101.1	1.627	54.085	3.535	1.131
1996	193	2.132	993.921	109.592	19.313
1997	79.8	1.556	99.392	2.313	1.126
1998	100.3	1.661	770.218	12.514	1.870
1999	298.5	2.229	1067.545	833.119	26.843
2000	95.5	1.498	181.511	3.519	1.230
2005	91.2	1.449	199.067	3.338	1.159
2006	110.2	1.767	276.089	6.834	2.181
2007	71.6	1.619	20.247	2.136	1.006
2008	104.1	2.036	600.317	27.667	3.062
2009	96.5	1.909	407.763	11.141	2.200
2010	78.7	1.833	438.911	7.837	1.410
2011	62.2	1.597	42.192	1.971	1.018
2012	94.5	1.463	90.048	2.786	1.112
2013	64.8	1.617	515.367	6.754	1.107
2014	94.2	1.749	36.246	3.936	1.071
2015	117.3	2.082	546.515	50.543	4.424
2016	1.866	172.733	10.185	1.970	

4.4.3 Regional Trivariate Comparison

To determine regional differences between occurrence of CCWE within the study region, the trivariate return period will be used to represent the probability of all drivers occurring at one time. To first represent the distribution at each station quantiles are determined (Table 4.17). The quantile, which is a measure of dispersion and variability, is shown as four equal parts, each being 1/4th of the entire range of the dataset (McGrew Jr. and Monroe,

2009). The first quantile represents the lowest 25% of the return period distribution while the fourth quantile represents the largest 25% of the return period distribution. The most-used quantiles are the 0% and 100% quantiles which are equivalent to the minimum and maximum respectively, while the 50% quantile represents the median.

To determine the regionality between the probability of occurrence of CCWE between all three case study locations, the distributions of trivariate return periods are compared. It was found through the Two-sample Kolmogorov-Smirnov test that all of the stations trivariate return periods are statistically similar, meaning there is not a statistically significant difference between all locations. Though the estimator of the CDF graphic shows that these central and southern study areas have the most similar shaped distribution which may be due to their similarity in geography compared to the northern region which is characterized by a large estuary environment. The area which may be at most risk to CCWE is the southern case study area as it has the "lowest" return periods which means that CCWE may occur more frequently based on our definition. In table 4.17, the southern case study has 50% of trivariate (T_{PTS}^{AND}) under 3.5 years.

Table 4.17: Trivariate return period quantiles for distributions of trivariate return periods for all case study areas.

	Quantile of Trivariate Return Period (years)				
Region	0%	25%	50%	75%	100%
Northern	1.299	2.443	5.346	13.434	400.026
Central	1.406	2.339	4.753	9.358	259.770
Southern	1.271	2.671	3.594	7.738	833.119

The objective of the Kolmogorov-Smirnov (K-S) statistic is to compare random sample frequency counts of a single variable with expected frequency counts. The K-S test tests similarity between two distributions. The K-S test is related to the comparison of the ECDFs associated to each population (Figure 4.16). The null hypothesis of this test states that no significant difference exists between the two frequency distributions. The K-S test statistic,

D, represents the maximum absolute difference between the two sets of cumulative values. When the deviation between the distributions is large, D is large and the null hypothesis of no difference between the two distributions could be incorrect. Conversely, if all the differences between the distributions are small, then D will be small and the distributions are statistically similar (McGrew Jr. and Monroe, 2009). Since the p-value between all case study pairs is greater than .05 (Table 4.18), we accept the null hypothesis. We have sufficient evidence to say that the three data sets come from similar distributions. It was found through the Two-sample Kolmogorov-Smirnov test that all of the stations trivariate return periods are statistically similar, meaning there is not a statistically significant difference between all locations.

Table 4.18: Two-sample kolmogorov-smirnov test for distributions of trivariate return periods for all case study areas.

Case Study Pair	K-S Test Statistic (D)	p-value
Northern-Central	0.15546	0.727
Northern-Southern	0.18824	0.5435
Central-Southern	0.17143	0.662

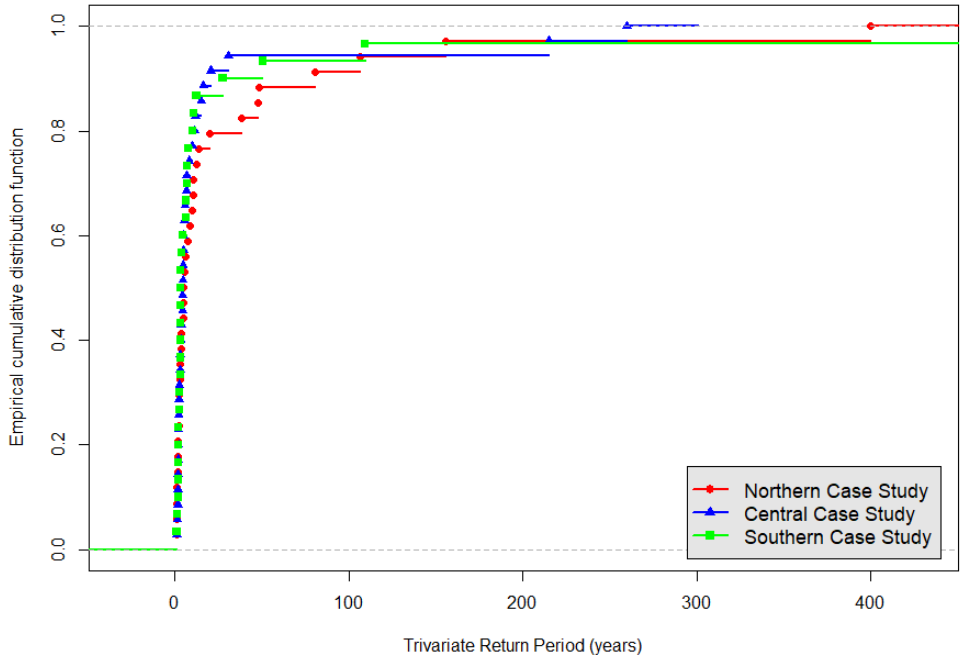

Figure 4.16: Comparing empirical cumulative distribution functions of trivariate return periods for all case study areas.

4.5 Focus Group Analysis

This section provides a review of focus group discussions and a pre-focus group survey to summarize perceptions of flood drivers among focus group participants. This builds upon the work of Mukherji et al. (2021b). The questions and results of the pre-focus group survey are within Appendix B. It was noted in depth how floods are high risk events that can occur year-round for some regions in Eastern North Carolina which can lead to health and infrastructure hazards. Attendees also emphasized the importance of rain as a driver of CCWE and the compounding aspects of risks that can be exacerbated by infrastructural deficiencies.

4.5.1 Relationships Between CCWE Drivers Perceptions

As just the quantitative analysis can explain the numerical results and relationships of the CCWE drivers, working with stakeholders we are able to further understand the path of occurrence, as well as relationship of drivers within CCWE. Participants elaborated upon how rain first falls and its impact is then seen within the rivers. At the same time impacts are seen from storm surge pushing up the river.

> *Over nine inches of rain, we know we're gonna have problems... once the rain falls, they have issues with it getting to the river, and once it gets to the river then the river swells. And then if we're in the middle of a hurricane and we've got coastal surge going on, then our river can't flush out. So all three of them really tie into what the issues are for everybody in the county.*

Though the attendees also noted, rain and riverine flooding are the most frequent and related, as well as most likely to combine into compound floods over common areas. Within the Pamlico Sound, which is within the Northern Case Study of this analysis participants said they "had storm surge coming up through Pamlico Sound... and in some cases close to fifty inches of rain upriver. So now were getting it from both sides." This was also noted in the Central Case Study area where New Bern, North Carolina is located,

> *New Bern had all of that wind pushing it up the river, and then after the storm kind of turned and set down over Wilmington, then you had all the water coming down the river. And that just compounded everything.*

4.5.2 Flood Hazard Perceptions

Emergency managers and planners who attended the workshop were asked how they perceive flood risk in their community or jurisdiction in regard to how often it occurs, the severity, and its comparison to other hazards. The consensus was that it is high to very high risk, as one participant noted,

We perceive flood risk in Bertie County, and Windsor included, as high, for us. I mean, take in seventeen years, we've had four one-hundred, five-hundred year floods, depending on who wants to calculate the risk of that.

This perception of the high level of risk is accompanied by the perception that flood hazards are growing in both severity and frequently. This was shown in both the pre-focus group survey and focus group discussions. In the pre-focus group survey, between all types of flooding, 80% of the participants saw pluvial as becoming more frequent than fluvial or tidal (Figure 4.17). In the focus group discussion, pluvial flooding was also the most unexpected form of flooding which is also becoming more surprising over the past 10 years. One participant told us, "over time, too, that the risk is starting to change, that its' not just what's in that mapped floodplain. We're running into a lot of localized flooding". It was stated that both tropical systems and heavy rainfall events are contributing to the high risk of flooding. Another participant stated how intensity and frequency are becoming more noticeable.

I think the intensity and the occurrence have both increased over the last twenty years. Used to, we dealt with flooding during a hurricane event most of the time and now you're getting a lot of localized flooding from a six-inch rain in the middle of the summer, which used to was unheard of.

In regard to frequency, the time between flood events is important to decision makers. Another aspect being that water tables become saturated (or impermeable) with recurring summer storms exacerbating impacts. Consecutive storms may make recovery more difficult as one participant notes, "You can't get one storm cleaned up before you've got another one." The threat of flooding is constant and clear. Municipal agencies frequently struggle recovering from one flood before being subjected to another.

It just seems like these hurricane keep rolling in. You might get a one-year reprieve but its every other year, it seems like, it's automatic.

Another question posed to the attendees is the type or source of flooding which is most surprising and unexpected in their community or jurisdiction. The types were ocean-caused, rain-caused, or river-caused which are the same drivers used in the analysis of CCWE. In both the pre-focus group survey and focus group discussions rain-caused floods are the most surprising, where there are concentrated areas of precipitation outside of established flood zones. To put this into perspective, one participant noted, "The storm we had three weeks ago was worse than the hurricane last October." The surprising aspect includes places unaccustomed to flooding now become flooded from rainstorms.

> *"But I think every big event ... for a typical rainstorm, we kind of know the rain flow. But when you get one of those mega-rainfalls, I don't know why but it floods in places that we're not accustomed to it flooding."*

Figure 4.17: Pre-focus group question: In the past 10 years, have these floods become more or less frequent?

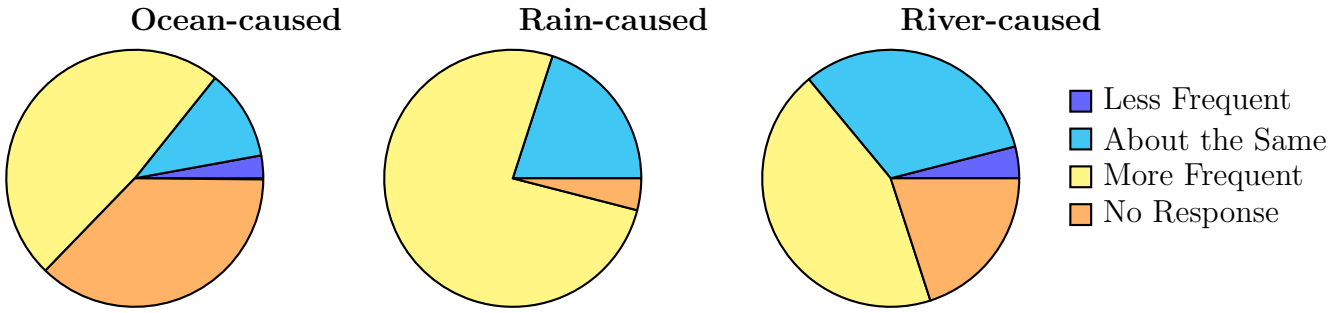

Similarly to asking about what type or source of flooding is most surprising, the participants were asked which is most damaging. The compounding nature of CCWE is a major contributor to impacts. Within the pre-focus group survey it was evident that for all drivers, the amount of damage has either stayed the same or increased when viewed separately (Figure 4.18. Compound flooding events incur compounding damages that can be difficult to evaluate individually. Storm surge, riverine flooding, and excessive rainfall can all damage property and infrastructure, but compound flooding increases and magnifies all damage.

It's causing damage more frequently, not necessarily causing more damage in one particular event. But because it's compounding each time it happens... it's definitely more damaging from that perspective.

Figure 4.18: Pre-focus group question: In the past 10 years have these floods become more or less damaging?

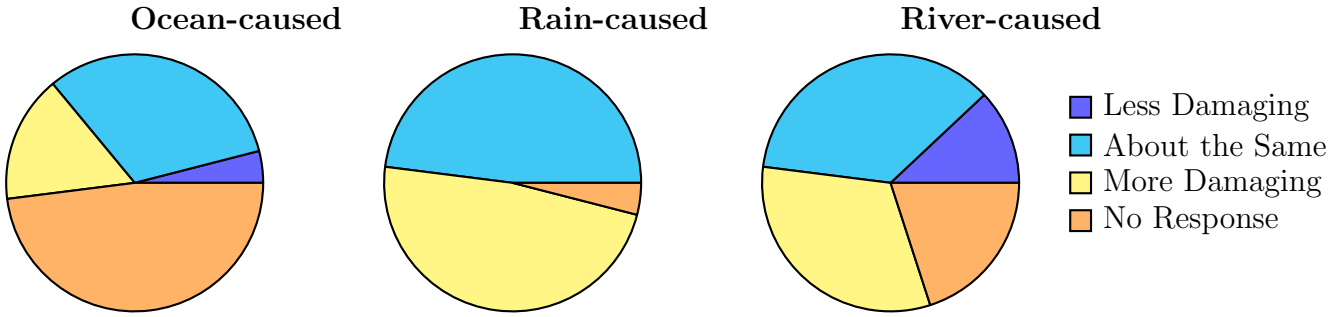

5 DISCUSSION AND CONCLUSION

This research investigates the relationships and return periods of drivers of Compound Coastal Water Events (CCWE) in Eastern North Carolina (NC) through use of copula modelling. The results display return periods of observed CCWE. The results of this analysis show that the occurrence of the drivers of equaling or exceeding a value simultaneously is less frequent in the "AND" case return periods compared to the "OR" case return periods. It is rarer to experience all three simultaneously than at least one occurring.

5.1 Discussion of Results

Within this research a definition of CCWE was constructed and events were located for three different case study locations within Eastern NC. The definition of CCWE was based upon the assumption that pluvial flooding was the primary driver of CCWE which was confirmed by the correlation structure between it and the other flooding types of tidal and fluvial. The strongest dependence is between the proxy for pluvial flooding: 24-hour precipitation ($millimeter$), and the proxy for tidal flooding: tide level above MLLW ($meter$). The second strongest dependence is between precipitation and the proxy for fluvial flooding: stream discharge (m^3/s). This highlights the contention that extreme precipitation is an important variable that needs to be incorporated into the analysis of CCWE. Another thing noted about the drivers are that their distributions are right or positively skewed, which is typically shown in the case of extreme events where more intense values are not as common as moderate or low values. In further interpreting what is a defined as a CCWE, all three locations exhibit CCWE with a minimum near 50 $millimeters$ of precipitation (i.e., northern case study: 48.3 $millimeters$, central case study: 47 $millimeters$, and southern case study: 56.1 $millimeters$).

One of the advantages of using copulas is you are able to create simulations of events from the distributions of drivers and modelled relationships. In all of the case study areas

copulas were fitted and showed agreement to empirical distributions of CCWE. It was established for the region of Eastern North Carolina that the copula method is an effective tool for multivariate modelling of CCWE, as the copula effectively preserved the dependence structure of multiple flood drivers. This dependence structure showed agreement within the theoretical univariate distributions and the copula simulated CCWE distributions.

From the copula simulations, the sample of CCWE is expanded and more return periods can be created to represent a broader probability of occurrence. Before examining the probability of occurrence for all variables occurring at the same time, univariate return periods were calculated to determine the probability of occurrence for observed measurements on their own. To further understand the relationship between drivers, trivariate return period were constructed to see the probability in the instance that of all three of the measurements occur at the same time. Two types of trivariate return periods were created. The first is the "OR" case which characterizes the probability that as least of the driver values will meet or exceed their value measured for that CCWE. The next type of trivariate return period is the "AND" case, which is the representation of how often it would be expected that all driver values in a CCWE meet or exceed their measurements within one event. Regarding the trivariate return periods, the "OR" case is always less than the return period for the "AND" cases. This is also interpreted as the occurrence of the drivers of interest equalling or exceeding a value simultaneously is less frequent in the "AND" compared to the "OR" case. It is more rare to see all together than at least one occurring. The comparative analysis of different return period types showed that is it important to calculate it in the trivariate sense to know the expected risk of CCWE and their potential probability of occurrence if they happen simultaneously.

Another aspect to consider with the return periods is comparing the univariate to trivariate outputs. For most cases in all case study areas, CCWE risk would be underestimated if each drivers univariate return period is added together compared to the return period derived from the trivariate copula models. If decision makers only consider the risk posed by

one driver compared to the risk posed by all drivers, they will underestimate the probability of the event occurring.

Within this project another goal is to connect the outcome from the statistical analysis to the discussions with decision makers which occurred at the focus group. Contributing to our motivation for this research, in both the pre-workshop survey and focus group discussions the participants noted that precipitation based flooding was becoming more frequent and more damaging. Participants also noted ways in which all three drivers are compounding adding more depth to the definition of CCWE. The perception held by decision makers reinforces the importance of considering pluvial flooding as a principal driver of CCWE in hazard and risk assessments.

5.2 Implications of Research

The results of this study add to our knowledge about Compound Coastal Water Events (CCWW) in Eastern North Carolina. Also, it was concluded that utilizing a copula model effectively preserves the dependence between CCWE drivers within events based upon simulated values and is thus a valuable tool for assessment of these multivariate events. From these copula models further simulations can be created from a limited temporal record dataset. This research will be shared directly with decision makers in a second focus group discussion as part of the National Oceanic and Atmospheric Administration (NOAA) Coastal Ocean Climate Applications (COCA)/Sectoral Applications Research Program (SARP) project: "Preparing for, Responding to, and Mitigating Compound Coastal Water Hazards for Resilient Rural Communities". As extreme impacts caused by tropical cyclones highlight the significance of compound events, communicating more accurate return periods that consider all variables will assist practitioners in planning.

5.3 Limitations of the Research

While this paper provides some important methodology and results, there are some limitations that must be noted. In researching compound flooding, only a few studies have explicitly tried to measure the impacts and risks given some practical difficulties in quantifying them. Some of these difficulties lie in spatial analysis as well as the number of variables added into the analysis. The copula model and return period output is only relevant to the three studied locations and cannot be generalized to all locations in which Compound Coastal Water Events (CCWE) occur. In using only in-situ stations this study was only limited to three locations given there were only this amount of tidal gauge stations within the region of study that fit the temporal record criteria. In addition to the location aspect, there are limitations and uncertainties involved with the formation of CCWE which may include additional flood drivers, flood protection structures, and catchment properties that affect water levels. Also, in creating return periods, the results are only related to the empirical CCWE values and not standardized years as typically presented to practitioners (i.e., 50, 100, 200 years). Another limitation is that this study is based on the assumption that the precipitation series is stationarity, even though this may not be true within a changing climate. Therefore, future studies should consider non-stationarity of precipitation and incorporate climate dynamics models. Also, the limited length of study period leads to the scarcity of the CCWE events, which is a major source of uncertainty in frequency analysis, particularly in the upper tail of the probability distributions. However, the CCWE frequency analysis method proposed in this study is beneficial for risk management.

5.4 Contributions to Knowledge and Future Work

This project has set a foundation for analyzing the co-occurrence of three flood hazards, that when they occur create a Compound Coastal Water Event (CCWE). This project utilizes and builds upon this term first introduced by Curtis and De Polt (2020). Future

work could extend this methodology to other coastal locations to further delve into spatial differences, which is similar to research question 2 posed within the introduction. Future work could also analyze more than one compound coastal water event per year. Seasonality would be an interesting approach so that different modes of precipitation-based hazards could be analyzed. As posed by Couasnon et al. (2020) further studies should investigate additional synoptic and meteorological aspects of these events, like the type of synoptic weather conditions. As with most compound events and hazards in general, flood events are extremely multidimensional, but can also be influenced by the different topography, land cover, human interventions, and water management.

5.5 Conclusion

There has been a paradigm shift in the understanding that most climate and weather events are composed of multiple hazards. These types of climate and weather events are defined as compound events. The paradigm shift is especially noticeable in the recent Intergovernmental Panel on Climate Change (Seneviratne et al., 2021) report where compound events were provided their own chapter in the physical science basis report. The goal of this project is to contribute to this ongoing paradigm shift and analyze a type of compound event. Within the study region of Eastern North Carolina, coastal floods are typically classified by three different flooding types: pluvial (i.e., precipitation-based), fluvial (i.e., river-based), and tidal (i.e., ocean-based). Especially during tropical cyclone events, which are a common occurrence within this region, these three flood types can occur within the time and place. When this occurs it is defined as a Compound Coastal Water Event (CCWE).

Typically in predicting, assessing, and researching these floods only one or two variables are considered. Utilizing these conventional univariate approaches will not give accurate information regarding the multivariate relationships and association impacts. The objectives of this thesis was to determine the trivariate relationship between the drivers of CCWE, find differences in regionality to these relationships, and determine if the perceptions that decision

makers in the region match the statistical interpretations. The methodology chosen, based upon previous literature, was the copula model. Copulas are useful in that the model can be created with unique marginal distribution representations for each variable. From modelled copulas simulated events can be created. These simulated events expand upon the limited temporal record of about 30 years for each of our case study locations. The relationships were compared to views and concerns held by decision makers within the study region, with data sourced from a focus group and accompanying survey.

By increasing the analysis from a traditional univariate or bivariate to a trivariate approach there will be a more complete depiction of compound coastal water events. Through this depiction the inclusion of more variables will lead to a more accurate risk assessment and return period. The findings in this study were connected to a survey and dialogue from a flood focus group. The focus group pre-workshop survey and discussions were able to provide key understanding about decision makers perceptions of CCWE hazards and relationships between drivers. To decision makers within the region believe that they are at a high level of risk from CCWE given it's increase in severity and frequency. Focus group participants also noted and reinforced the concept found within the copula modelled analysis that precipitation is one of the most important drivers of CCWE. It will be important in future correspondence to convey to decision makers the importance of CCWE with extreme precipitation along with corresponding high tidal levels and stream discharge. While the results of this analysis have established new understanding there are even more spatial and temporal research pursuits which may be undertaken.

REFERENCES

AghaKouchak, A., Huning, L. S., Chiang, F., Sadegh, M., Vahedifard, F., Mazdiyasni, O., Moftakhari, H., and Mallakpour, I. (2018). How do natural hazards cascade to cause disasters? *Nature*, 561:458–460.

Akaike, H. (1973). Information theory and an extension of the maximum likelihood principle. In *Proc. 2nd Inter. Symposium on Information Theory*, pages 267–281.

Alfieri, L., Salamon, P., Bianchi, A., Neal, J., Bates, P., and Feyen, L. (2014). Advances in pan-european flood hazard mapping. *Hydrol. Process.*, 28(13):4067–4077.

Apel, H., Martínez Trepat, O., Hung, N. N., Chinh, D. T., Merz, B., and Dung, N. V. (2016). Combined fluvial and pluvial urban flood hazard analysis: concept development and application to can tho city, mekong delta, vietnam. *Nat. Hazards Earth Syst. Sci.*, 16:941–961.

Archetti, R., Bolognesi, A., Casadio, A., and Maglionico, M. (2011). Development of flood probability charts for urban drainage network in coastal areas through a simplified joint assessment approach. *Hydrol. Earth Syst. Sci.*, 15:3115–3122.

Balistrocchi, M. and Bacchi, B. (2011). Modelling the statistical dependence of rainfall event variables through copula functions. *Hydrol. Earth Syst. Sci.*, 15:1959–1977.

Bevacqua, E., Maraun, D., Vousdoukas, M. I., Voukouvalas, E., Vrac, M., Mentaschi, L., and Widmann, M. (2019). Higher probability of compound flooding from precipitation and storm surge in europe under anthropogenic climate change. *Sci. Adv.*, 5(9).

Bezak, N., Mikoš, M., and Šraj, M. (2014). Trivariate frequency analyses of peak discharge, hydrograph volume and suspended sediment concentration data using copulas. *Water Resour. Manage.*, 28:2195–2212.

Blanchard, B. W. (2018). *Guide to Emergency Management and Related Terms, Definitions, Concepts, Acronyms, Organizations, Programs, Guidance, Executive Orders & Legislation: A Tutorial on Emergency Management, Broadly Defined, Past and Present.* Federal Emergency Management Agency.

Brewer, M. J., Butler, A., and Cooksley, S. L. (2016). The relative performance of aic, aicc and bic in the presence of unobserved heterogeneity. *Methods Ecol. Evol.*, 7(6):679–692.

Brown, S., Nicholls, R. J., Lowe, J. A., and Hinkel, J. (2016). Spatial variations of sea-level rise and impacts: An application of diva. *Climatic Change*, 134:403–416.

Bulla, B. R., Craig, E. A., and Steelman, T. A. (2017). Climate change and adaptive decision making: Responses from north carolina coastal officials. *Ocean Coast. Manage.*, 135:25–33.

Buschman, F. A., Hoitink, A. J. F., van der Vegt, M., and Hoekstra, P. (2019). Subtidal water level variation controlled by river flow and tides. *Water Resour. Res.*, 45(10).

Castrucci, L. and Tahvildari, N. (2018). Modeling the impacts of sea level rise on storm surge inundation in flood-prone urban areas of hampton roads, virginia. *Mar. Technol. Soc. J.*, 52(2):92–105.

Chen, L., Guo, S., Yan, B., Liu, P., and Fang, B. (2010). A new seasonal design flood method based on bivariate joint distribution of flood magnitude and date of occurrence. *Hydrolog. Sci. J.*, 55(8):1264–1280.

Chen, L., Singh, V. P., Shenglian, G., Hao, Z., and Li, T. (2012). Flood coincidence risk analysis using multivariate copula functions. *J. Hydrol. Eng.*, 17(6):742–755.

Couasnon, A., Eilander, D., Muis, S., Veldkamp, T. I. E., Haigh, I. D., Wahl, T., Winsemius, H. C., and Ward, P. J. (2020). Measuring compound flood potential from river discharge and storm surge extremes at the global scale. *Nat. Hazards Earth Syst. Sci.*, 20(2):489–504.

Curtis, S. and De Polt, K. (2020). Compound coastal water events from 1980 to 2018 in eastern north carolina.

De Michele, C. and Salvadori, G. (2003). A generalized pareto intensity-duration model of storm rainfall exploiting 2-copulas. *J. Geophys. Res.-Atmos.*, 108(D2).

De Michele, C., Salvadori, G., Canossi, M., Petaccia, A., and Rosso, R. (2005). Bivariate statistical approach to check adequacy of dam spillway. *J. Hydrol. Eng.*, 10(1):50–57.

Dottori, F., Salamon, P., Bianchi, A., Alfieri, L., Hirpa, F. A., and Feyen, L. (2016). Development and evaluation of a framework for global flood hazard mapping. *Adv. Water Resour.*, 94:87–102.

Escalante Sandoval, C. and Raynal-Villaseñor, J. (2008). Trivariate generalized extreme value distribution in flood frequency analysis. *Hydrolog. Sci. J.*, 53(3):550–567.

Escalante Sandoval, C. A. and Raynal-Villasenor, J. (1994). A trivariate extreme value distribution applied to flood frequency analysis. *J. Res. Natl. Inst. Stan.*, 99(4):369–375.

Ezer, T. and Atkinson, L. P. (2014). Accelerated flooding along the u.s. east coast: On the impact of sea-level rise, tides, storms, the gulf stream, and the north atlantic oscillations. *Earths Future*, 2(8):362–382.

Favre, A.-C., El Adlouni, S., Perreault, L., Thiémonge, N., and Bobée, B. (2004). Multivariate hydrological frequency analysis using copulas. *Water Resour. Res.*, 40(1).

Federal Emergency Management Agency (2020). Guidance for flood risk analysis and mapping: Combined coastal and riverine floodplain. Technical report, Federal Emergency Management Agency.

Ganguli, P. and Reddy, M. J. (2013). Probabilistic assessment of flood risks using trivariate copulas. *Theor. Appl. Climatol.*, 111:341–360.

Genest, C. and Favre, A.-C. (2007). Everything you always wanted to know about copula modeling but were afraid to ask. *J. Hydrol. Eng.*, 12:347–368.

Genest, C., Rémillard, B., and Beaudoin, D. (2009). Goodness-of-fit tests for copulas: A review and a power study. *Insur. Math. Econ.*, 44(2):199–213.

Grimaldi, S. and Serinaldi, F. (2006). Asymmetric copula in multivariate flood frequency analysis. *Adv. Water Resour.*, 29(8):1155–1167.

Gräler, B., van den Berg, M., Vandenberg, S., Petroselli, A., Grimaldi, S., De Baets, B., and Verhoest, N. E. C. (2013). Multivariate return periods in hydrology: a critical and practical review focusing on synthetic design hydrograph estimation. *Hydrol. Earth Syst. Sci.*, 17:1281–1296.

Gumbel, E. J. (1958). *Statistics of Extremes*. Columbia University Press, New York.

Hendry, A., Haigh, I. D., Nicholls, R. J., Winter, H., Neal, R., Wahl, T., Joly-Laugel, A., and Darby, S. E. (2019). Assessing the characteristics and drivers of compound flooding events around the uk coast. *Hydrol. Earth Syst. Sci.*, 23(7):3117–3139.

Hinkel, J., Lincke, D., Vafeidis, A. T., Perrette, M., Nicholls, R. J., Tol, R. S. J., Marzeion, B., Fettweis, X., Ionescu, C., and Levermann, A. (2014). Coastal flood damage and adaptation costs under 21st century sea-level rise. *P. Natl. Acad. Sci. USA*, 111(9):3292–3297.

Hirabayashi, Y., Mahendran, R., Koirala, S., Konoshima, L., Yamazaki, D., Watanabe, S., Kim, H., and Kanae, S. (2013). Global flood risk under climate change. *Nat. Clim. Change*, 3:816–821.

Hirschboeck, K. K., Ely, L. I., and Maddox, R. A. (2000). Hydroclimatology of meteorologic floods. In Wohl, E. E., editor, *Inland Flood Hazards: Human, Riparian and Aquatic Communities*, chapter 1, pages 39–72. Cambridge University Press, New York.

Jaeger, C. C., Webler, T., Rosa, E. A., and Renn, O. (2001). *Risk, Uncertainty and Rational Action*. Earthscan Risk in Society. Routledge, London, United Kingdom, 1st edition.

Jasim, F. H., Vahedifard, F., Alborzi, A., Moftakhari, H., and AghaKouchak, A. (2020). Effect of compound flooding on performance of earthen levees. In *Geo-Congress 2020: Engineering, Monitoring, and Management of Geotechnical Infrastructure*, Reston, Virginia. American Society of Civil Engineers.

Joe, H. (1997). *Multivariate Models and Multivariate Dependence Concepts*. Chapman and Hall/CRC Press, New York, 1st edition.

Karamouz, M., Nazif, S., and Falahi, M. (2013). *Hydrology and Hydroclimatology : Principles and Applications*. CRC Press, Boca Raton.

Kew, S. F., Selten, F. M., Lenderink, G., and Hazeleger, W. (2013). The simultaneous occurrence of surge and discharge extremes for the rhine delta. *Nat. Hazards Earth Syst. Sci.*, 13(8):2017–2029.

Khanal, S., Ridder, N., de Vries, H., Terink, W., and van den Hurk, B. (2019). Storm surge and extreme river discharge: A compound event analysis using ensemble impact modeling. *Front. Earth Sci.*, 7:1–15.

Klerk, W. J., Winsemius, H. C., van Verseveld, W. J., Bakker, A. M. R., and Diermanse, F. L. M. (2015). The co-incidence of storm surges and extreme discharges within the rhine–meuse delta. *Environ. Res. Lett.*, 10(035005).

Kumbier, K., Carvalho, R. C., Vafeidis, A. T., and Woodroffe, C. D. (2018). Investigating compound flooding in an estuary using hydrodynamic modelling: a case study from the shoalhaven river, australia. *Nat. Hazard Earth Sys.*, 18(2):463–477.

Latif, S. and Mustafa, F. (2020). Trivariate distribution modelling of flood characteristics using copula function—a case study for kelantan river basin in malaysia. *AIMS Geosciences*, 6(1):92–130.

Leonard, M., Westra, S., Phatak, A., Lambert, M., van den Hurk, B., McInnes, K., Risbey, J., Schuster, S., Jakob, D., and Stafford-Smith, M. (2014). A compound event framework for understanding extreme impacts. *WIREs Clim. Change*, 5(1):113–128.

Liebscher, E. (2008). Construction of asymmetric multivariate copulas. *J. Multivariate Anal.*, 99(10):2234–2250.

McEntire, D. A. (2018). *Learning More About the Emergency Management Professional*. FEMA Higher Education Program.

McGrew Jr., J. C. and Monroe, C. B. (2009). *An Introduction to Statisical Problem Solving in Geography*. Waveland Pr Inc, Long Grove, Ilinois, 2nd edition.

Miles, M. B. and Huberman, A. M. (1994). *An expanded sourcebook: Qualitative data analysis*. Sage Publications, London.

Moftakhari, H., Schubert, J. E., AghaKouchak, A., Matthew, R., and Sanders, B. F. (2019). Linking statistical and hydrodynamic modeling for compound flood hazard assessment in tidal channels and estuaries. *Adv. Water Resour*, 128:28–38.

Moftakhari, H. R., Salvadori, G., AghaKouchak, A., Sanders, B. F., and Matthew, R. A. (2017). Compounding effects of sea level rise and fluvial flooding. *PNAS*, 114(37):9785–9785.

Muis, S., Verlaan, M., Winsemius, H. C., Aerts, J. C. J. H., and Ward, P. J. (2016). A global reanalysis of storm surges and extreme sea levels. *Nat. Commun.*, 7(11969).

Mukherji, A., Curtis, S., Van Wagoner, P., Kruse, J., Helgeson, J., and Ghosh, A.and De Polt, K. (2021a). Mitigating water hazards in eastern north carolina: Perspectives of planners and emergency managers. Association of the Collegiate Schools of Planning Conference, Virtual Event, October 7, 2021.

Mukherji, A., Van Wagoner, P., Curtis, S., Kruse, J., Helgeson, J., and DePolt, K. (2021b). Planning for resilience: An analysis of compound flooding in eastern north carolina. Carolinas Climate Resilience Conference, Chapel Hill, North Carolina, May 11, 2021.

National Research Council (2011). Building community disaster resilience through private-public collaboration. Technical report, The National Academies Press, Washington, DC.

National Research Council (2012). Disaster resilience: A national imperative. Technical report, The National Academies Press, Washington, DC.

Nelsen, R. B. (2006). *An Introduction to Copulas*. Springer Series in Statistics. Springer-Verlag, New York.

NOAA National Hurricane Center (2021). Tropical cyclone climatology. `https://www.nhc.noaa.gov/climo/`. Last checked on Nov 01, 2013.

Olbert, A. I., Comer, J., Nash, S., and Hartnett, M. (2017). High-resolution multi-scale modelling of coastal flooding due to tides, storm surges and rivers inflows. a cork city example. *Coast. Eng.*, 121:278–296.

Paerl, H. W., Hall, N. S., Hounshell, A. G., Jr., R. A. L., Rossignol, K. L., Osburn, C. L., and Bales, J. (2019). Recent increase in catastrophic tropical cyclone flooding in coastal north carolina, usa: Long-term observations suggest a regime shift. *Scientific Reports*, 9.

Pasch, R. J., Kimberlain, T. B., and Stewart, S. R. (1999). Preliminary report: Hurricane floyd. Technical report, National Hurricane Center.

Ramachandran, K. M. and Tsokos, C. P. (2020). *Mathematical Statistics with Applications in R*. Academic Press, 3rd edition.

Resio, D. T. and Westerink, J. J. (2008). Modeling the physics of storm surges. *Physics Today*, 61:33–38.

Sadegh, M., Moftakhari, H., Gupta, H. V., Ragno, E., Mazdiyasni, O., Sanders, B., Matthew, R., and AghaKouchak, A. (2018). Multihazard scenarios for analysis of compound extreme events. *Geophys. Res. Lett.*, 45(11):5470–5480.

Saldana, J. (2009). *The coding manual for qualitative researchers*. Sage Publications Ltd, Los Angeles.

Salvadori, G. (2004). Bivariate return periods via-2 copulas. *Stat. Methodol.*, 1:129–144.

Salvadori, G. and De Michele, C. (2004). Frequency analysis via copulas: Theoretical aspects and applications to hydrological events. *Water Resour. Res.*, 40(12).

Salvadori, G., Durante, F., De Michele, C., Bernardi, M., , and Petrella, L. (2016). A multivariate copula-based framework for dealing with hazard scenarios and failure probabilities. *Water Resour. Res.*, 52(5):3701–3721.

Salvadori, G., Tomasicchio, G. R., and D'Alessandro, F. (2014). Practical guidelines for multivariate analysis and design in coastal and off-shore engineering. *Coastal Engineering*, 88:1–14.

Schaffer-Smith, D., Myint, S. W., Muenich, R. L., Tong, D., and DeMeester, J. E. (2020). Repeated hurricanes reveal risks and opportunities for social-ecological resilience to flooding and water quality problems. *Environmental Science & Technology*, 54(12):7194–7204.

Seneviratne, S. I., Zhang, X., Adnan, M., Badi, W., Dereczynski, C., Di Luca, A., Ghosh, S., Iskandar, I., Kossin, J., Lewis, S., Otto, F., Pinto, I., Satoh, M., Vicente-Serrano, S. M., Wehner, M., and Zhou, B. (2021). Weather and climate extreme events in a changing climate. In *2021: Climate Change 2021: The Physical Science Basis. Contribution of Working Group I to the Sixth Assessment Report of the Intergovernmental Panel on Climate Change*, chapter 11. Cambridge University Press.

Stewart, S. R. (2017). Tropical cyclone report hurricane matthew. Technical report, National Hurricane Center.

Stewart, S. R. and Berg, R. (2019). Tropical cyclone report hurricane florence. Technical report, National Hurricane Center.

Svensson, C. and Jones, D. A. (2002). Dependence between extreme sea surge, river flow and precipitation in eastern britain. *Int. J. Climatol.*, 22:1149–1168.

Svensson, C. and Jones, D. A. (2004). Dependence between sea surge, river flow and precipitation in south and west britain. *Int. J. Climatol.*, 8(5):973–992.

Teegavarapu, R. (2012). *Hydrology and Hydroclimatology : Principles and Applications*. Cambridge University Press, Cambridge.

Tierney, K. (2014). *The Social Roots of Risk: Producing Disasters, Promoting Resilience*. High Reliability and Crisis Management. Stanford University Press, Stanford, California.

Vousdoukas, M. I., Mentaschi, L., Voukouvalas, E., Bianchi, A., Dottori, F., and Feyen, L. (2018). Climatic and socioeconomic controls of future coastal flood risk in europe. *Nat. Clim. Chang.*, 8:776–780.

Wahl, T., Jain, S., Bender, J., Meyers, S. D., and Luther, M. E. (2015). Increasing risk of compound flooding from storm surge and rainfall for major us cities. *Nature Clim. Change*, 5:1093–1097.

Ward, P., Jongman, B., Weiland, F., Bouwman, A., van Beek, R., Bierkens, M., Ligtvoet, W., and Winsemius, H. (2013). Assessing flood risk at the global scale: Model setup, results, and sensitivity. *Environ. Res. Lett.*, 8.

Ward, P. J., Couasnon, A., Eilander, D., Haigh, I. D., Hendry, A., Muis, S., Veldkamp, T. I. E., Winsemius, H. C., and Thomas Wahl, T. (2018). Dependence between high sea-level and high river discharge increases flood hazard in global deltas and estuaries. *Environ. Res. Lett.*, 13(8).

Ward, P. J., Jongman, B., Aerts, J. C. J. H., Bates, P. D., Botzen, W. J. W., Diaz Loaiza, A., Hallegatte, S., Kind, J. M., Kwadijk, J., Scussolini, P., and Winsemius, H. C. (2017). A global framework for future costs and benefits of river-flood protection in urban areas. *Nat. Clim. Change*, 7:642–646.

Winsemius, H. C., Aerts, J. C. J. H., van Beek, L. P. H., Bierkens, M. F. P., Bouwman, A., Jongman, B., Kwadijk, J. C. J., Ligtvoet, W., Lucas, P. L., van Vuuren, D. P., and Ward, P. J. (2016). Global drivers of future river flood risk. *Nat. Clim. Change*, 6:381–385.

Winsemius, H. C., Van Beek, L. P. H., Jongman, B., Ward, P. J., and Bouwman, A. (2013). A framework for global river flood risk assessments. *Hydrol. Earth Syst. Sci.*, 17(5):1871–1892.

Wu, W., McInnes, K., O'Grady, J., Hoeke, R., Leonard, M., and Westra, S. (2018). Mapping dependence between extreme rainfall and storm surge. *J. Geophys. Res.-Oceans*, 123(4):2461–2474.

Zhang, L. and Singh, V. P. (2006). Bivariate flood frequency analysis using the copula method. *J. Hydrol. Eng.*, 11(2).

Zhang, L. and Singh, V. P. (2007). Trivariate flood frequency analysis using the gumbel–hougaard copula. *J. Hydrol. Eng.*, 12(4):431–439.

Zhang, L. and Singh, V. P. (2019). *Copulas and their Applications in Water Resources Engineering*. Cambridge University Press, Cambridge.

Zheng, F., Westra, S., and Sisson, S. A. (2013). Quantifying the dependence between extreme rainfall and storm surge in the coastal zone. *J. Hydrol.*, 505(15):172–187.

Zscheischler, J. and Fischer, E. M. (2020). The record-breaking compound hot and dry 2018 growing season in germany. *Weather Clim. Extremes*, 29.

Zscheischler, J., Westra, S., van den Hurk, B., Seneviratne, S. I., Ward, P. J., Pitman, W., AghaKouchak, A., Bresch, D. N., Leonard, M., Wahl, T., and Zhang, X. (2018). Future climate risk from compound events. *Nat. Clim. Change*, 8:469–477.

Zuccaro, G., De Gregorioa, D., and Leone, M. F. (2018). Theoretical model for cascading effects analyses. *Int. J. Disast. Risk Re.*, 30(B):199–215.

Appendix A: Compound Coastal Water Event Data

Northern study area CCWE events

Date of Max. Precip.	Precip. (mm)	Tide (m)	Date of Max. Tide	Stream (m^3/s)	Date of Max. Stream
9/6/1987	66	1.268	9/8/1987	0.039643585	9/8/1987
8/21/1988	67.3	1.122	8/24/1988	0.679604318	8/22/1988
7/13/1989	96.5	1.171	7/14/1989	0.16423771	7/16/1989
11/10/1990	49.5	1.271	11/10/1990	0.764554858	11/12/1990
7/11/1991	108	1.439	7/11/1991	5.635052472	7/14/1991
8/16/1992	57.2	1.256	8/16/1992	84.95053978	8/19/1992
3/13/1993	54.6	1.149	3/13/1993	14.72476023	3/15/1993
3/2/1994	115.6	1.442	3/4/1994	66.26142103	3/4/1994
6/6/1995	95.3	1.302	6/9/1995	9.599410995	6/8/1995
10/8/1996	140	1.417	10/9/1996	38.2277429	10/10/1996
8/20/1997	53.3	1.438	8/22/1997	0.003114853	8/21/1997
2/4/1998	55.9	1.762	2/5/1998	81.26934972	2/6/1998
9/16/1999	114.3	1.362	9/16/1999	410.5942756	9/17/1999
6/29/2000	115.8	1.422	7/2/2000	12.65763043	6/30/2000
7/27/2001	86.4	1.479	7/27/2001	14.63980969	7/28/2001
8/26/2002	66	1.24	8/29/2002	0.000566337	8/28/2002
9/18/2003	196.9	2.383	9/18/2003	93.44559375	9/20/2003
8/14/2004	48.3	1.24	8/17/2004	116.3822395	8/16/2004
10/8/2005	154.9	1.385	10/11/2005	16.45208787	10/10/2005
9/1/2006	128.5	1.44	9/3/2006	72.77429574	9/3/2006
8/22/2007	62.2	1.246	8/22/2007	0	2007-08-22, 2007-08-23, 2007-08-24, 2007-08-25
7/24/2008	57.7	1.147	7/26/2008	0.105338669	7/24/2008
11/12/2009	118.6	2.006	11/13/2009	20.84119909	11/14/2009
9/30/2010	124.2	1.521	10/3/2010	270.7090534	10/1/2010
8/27/2011	274.6	1.52	8/27/2011	114.9663972	8/28/2011
8/19/2012	82.6	1.49	8/20/2012	0.450237861	8/19/2012
10/10/2013	67.3	1.761	10/10/2013	0.351128898	10/13/2013
9/14/2014	74.9	1.494	9/14/2014	4.105942756	9/14/2014
6/26/2015	102.6	1.242	6/28/2015	0.235596164	6/26/2015
10/9/2016	215.9	1.647	10/9/2016	282.3189605	10/9/2016
6/6/2017	59.2	1.569	6/7/2017	2.511704293	6/8/2017
6/20/2018	72.4	1.342	6/23/2018	3.709506904	6/23/2018
9/6/2019	118.1	2.044	9/6/2019	8.353469745	9/7/2019
2/7/2020	94	1.616	2/7/2020	76.73865426	2/8/2020

Central study area CCWE events

Date of Max. Precip.	Precip. (mm)	Tide (m)	Date of Max. Tide	Stream (m^3/s)	Date of Max. Stream
3/29/1980	60.7	1.056	3/31/1980	51.81982926	4/1/1980
8/20/1981	99.1	1.319	8/22/1981	81.83568665	8/22/1981
1/4/1982	82.6	1.05	1/4/1982	32.56437358	1/6/1982
6/1/1983	89.2	1.044	6/1/1983	0.566336932	1983-06-01, 1983-06-02
2/14/1984	118.1	1.252	2/14/1984	41.34259602	2/16/1984
9/27/1985	122.4	1.636	9/27/1985	2.239862565	9/29/1985
8/19/1986	116.1	1.34	8/20/1986	33.13071051	8/22/1986
3/1/1987	52.8	1.267	3/1/1987	51.25349233	3/3/1987
6/10/1988	62.7	1.252	6/10/1988	3.567922671	6/12/1988
9/3/1989	61	1.157	9/6/1989	1.33089179	9/4/1989
3/30/1990	75.4	1.258	3/30/1990	26.24971679	4/2/1990
3/30/1991	74.7	1.215	3/30/1991	22.20040773	4/2/1991
8/14/1992	73.9	1.288	1992-08-17, 1992-08-17	50.97032387	8/17/1992
9/5/1993	50.5	1.096	1993-09-07, 1993-09-08	3.398021591	9/8/1993
10/14/1994	94	1.322	10/17/1994	44.74061762	10/16/1994
7/5/1995	50.3	1.227	7/8/1995	10.08079739	7/5/1995
9/6/1996	148.8	1.863	9/6/1996	56.91686165	9/9/1996
3/15/1997	47	1.021	3/15/1997	15.26278031	3/17/1997
8/27/1998	147.6	1.638	8/27/1998	37.66140597	8/30/1998
9/16/1999	273.6	1.915	9/16/1999	339.8021591	9/17/1999
9/19/2000	73.9	1.158	9/19/2000	13.19565051	9/21/2000
7/30/2001	92.2	1.203	8/1/2001	2.321981421	8/1/2001
3/3/2002	48.3	1.208	3/3/2002	37.3782375	3/6/2002
7/14/2003	137.9	1.186	7/15/2003	82.96836051	7/16/2003
10/14/2004	72.1	1.52	10/15/2004	3.82277429	10/17/2004
10/8/2005	156	1.546	10/8/2005	127.9921466	10/10/2005
9/1/2006	160.3	1.343	9/1/2006	225.4020989	9/3/2006
10/27/2007	68.6	1.562	10/27/2007	0.141017896	10/30/2007
9/26/2008	94.2	1.501	9/26/2008	1.713169219	9/28/2008
11/12/2009	111.5	1.755	11/14/2009	29.73268892	11/15/2009
9/30/2010	250.2	1.53	9/30/2010	124.8772935	10/2/2010
8/27/2011	153.7	1.905	8/27/2011	28.60001506	8/30/2011
7/13/2012	128.8	1.132	7/14/2012	8.72158875	7/16/2012
7/30/2013	80.8	1.094	8/2/2013	1.387525483	7/30/2013
7/4/2014	77.2	1.188	7/5/2014	5.720003012	7/6/2014

Southern study area CCWE events

Date of Max. Precip.	Precip. (mm)	Tide (m)	Date of Max. Tide	Stream (m^3/s)	Date of Max. Stream
8/17/1980	69.6	1.192	8/20/1980	25.62674617	8/20/1980
7/30/1981	123.7	1.566	8/1/1981	85.80004517	8/1/1981
10/25/1982	97.8	1.457	10/28/1982	174.7149435	10/28/1982
6/8/1983	105.4	1.679	6/11/1983	129.4079889	1983-06-09, 1983-06-11
7/14/1984	61.5	1.368	7/14/1984	216.9070449	7/17/1984
7/17/1985	59.2	1.56	7/19/1985	41.34259602	7/17/1985
5/20/1986	69.9	1.591	5/23/1986	60.03171478	5/22/1986
9/10/1987	71.6	1.502	9/10/1987	113.2673864	9/11/1987
1/8/1988	56.1	1.292	1/8/1988	294.4952046	1/8/1988
10/2/1989	85.3	1.509	10/2/1989	540.8517699	10/5/1989
8/8/1990	100.3	1.396	8/8/1990	78.72083353	8/11/1990
9/26/1991	97.8	1.472	9/28/1991	116.665408	9/28/1991
9/17/1993	101.1	1.627	9/19/1993	54.08517699	9/19/1993
9/6/1996	193	2.132	9/6/1996	993.9213154	9/9/1996
9/25/1997	79.8	1.556	9/28/1997	99.39213154	9/28/1997
3/9/1998	100.3	1.661	3/9/1998	770.2182273	3/12/1998
9/16/1999	298.5	2.229	9/16/1999	1067.545117	9/19/1999
9/5/2000	95.5	1.498	9/8/2000	181.5109867	9/6/2000
7/30/2005	91.2	1.449	8/2/2005	199.0674315	8/2/2005
9/1/2006	110.2	1.767	9/4/2006	276.0892543	9/2/2006
8/27/2007	71.6	1.619	8/30/2007	20.24654531	8/30/2007
9/6/2008	104.1	2.036	9/6/2008	600.3171478	9/9/2008
11/11/2009	96.5	1.909	11/14/2009	407.7625909	11/14/2009
9/30/2010	78.7	1.833	9/30/2010	438.9111222	10/3/2010
8/27/2011	62.2	1.597	8/30/2011	42.19210142	8/28/2011
7/12/2012	94.5	1.463	7/14/2012	90.04757216	7/15/2012
6/7/2013	64.8	1.617	6/7/2013	515.366608	6/10/2013
7/11/2014	94.2	1.749	7/14/2014	36.24556364	7/12/2014
10/3/2015	117.3	2.082	10/4/2015	546.5151392	10/6/2015
9/3/2016	123.2	1.866	9/3/2016	172.7327642	9/4/2016

Appendix B: Pre-Focus Group Survey

1. How frequent are the following types of floods?
    - Rain-caused
        - Never: 0 respondent(s)
        - Almost never: 1 respondent(s)
        - Somewhat frequent: 14 respondent(s)
        - Very frequent: 8 respondent(s)
        - Constant: 1 respondent(s)
        - Not applicable: 0 respondent(s)
        - No response: 1 respondent(s)
    - Ocean-caused
        - Never: 3 respondent(s)
        - Almost never: 1 respondent(s)
        - Somewhat frequent: 8 respondent(s)
        - Very frequent: 2 respondent(s)
        - Constant: 1 respondent(s)
        - Not applicable: 9 respondent(s)
        - No response: 1 respondent(s)
    - River-caused
        - Never: 1 respondent(s)
        - Almost never: 2 respondent(s)
        - Somewhat frequent: 14 respondent(s)
        - Very frequent: 3 respondent(s)
        - Constant: 1 respondent(s)
        - Not applicable: 3 respondent(s)
        - No response: 1 respondent(s)

2. In the past 10 years, have these floods become more or less frequent?
    - Rain-caused
        - Less frequent: 0 respondent(s)
        - About the same: 5 respondent(s)
        - More frequent: 19 respondent(s)
        - No response: 1 respondent(s)
    - Ocean-caused
        - Less frequent: 1 respondent(s)
        - About the same: 4 respondent(s)
        - More frequent: 7 respondent(s)
        - No response: 13 respondent(s)
    - River-caused
        - Less frequent: 1 respondent(s)
        - About the same: 8 respondent(s)
        - More frequent: 11 respondent(s)
        - No response: 5 respondent(s)

3. When are these types of floods surprising/unexpected?

    - Rain-caused
        - Never: 0 respondent(s)
        - Sometimes: 13 respondent(s)
        - About half the time: 4 respondent(s)
        - Most of the time: 6 respondent(s)
        - Always: 1 respondent(s)
        - Not applicable: 0 respondent(s)
        - No response: 1 respondent(s)
    - Ocean-caused
        - Never: 8 respondent(s)
        - Sometimes: 4 respondent(s)
        - About half the time: 2 respondent(s)
        - Most of the time: 0 respondent(s)
        - Always: 0 respondent(s)
        - Not applicable: 10 respondent(s)
        - No response: 1 respondent(s)
    - River-caused
        - Never: 5 respondent(s)
        - Sometimes: 14 respondent(s)
        - About half the time: 0 respondent(s)
        - Most of the time: 2 respondent(s)
        - Always: 0 respondent(s)
        - Not applicable: 3 respondent(s)
        - No response: 1 respondent(s)

4. In the past 10 years have these floods become more or less surprising?
    - Rain-caused
        - Less surprising: 8 respondent(s)
        - About the same: 9 respondent(s)
        - More surprising: 6 respondent(s)
        - No response: 2 respondent(s)
    - Ocean-caused
        - Less surprising: 2 respondent(s)
        - About the same: 10 respondent(s)
        - More surprising: 0 respondent(s)
        - No response: 13 respondent(s)
    - River-caused
        - Less surprising: 7 respondent(s)
        - About the same: 10 respondent(s)
        - More surprising: 2 respondent(s)
        - No response: 6 respondent(s)

5. How damaging are these types of floods?

    - Rain-caused
        - Not damaging: 1 respondent(s)
        - Slightly damaging: 6 respondent(s)
        - Somewhat damaging: 11 respondent(s)
        - Very damaging: 5 respondent(s)
        - Extremely damaging: 0 respondent(s)
        - Not applicable: 0 respondent(s)
        - No response: 1 respondent(s)
    - Ocean-caused
        - Not damaging: 1 respondent(s)
        - Slightly damaging: 1 respondent(s)
        - Somewhat damaging: 4 respondent(s)
        - Very damaging: 5 respondent(s)
        - Extremely damaging: 2 respondent(s)
        - Not applicable: 9 respondent(s)
        - No response: 3 respondent(s)
    - River-caused
        - Not damaging: 3 respondent(s)
        - Slightly damaging: 1 respondent(s)
        - Somewhat damaging: 2 respondent(s)
        - Very damaging: 9 respondent(s)
        - Extremely damaging: 5 respondent(s)
        - Not applicable: 4 respondent(s)
        - No response: 1 respondent(s)

6. In the past 10 years have these floods become more or less damaging?
    - Rain-caused
        - Less damaging: 0 respondent(s)
        - About the same: 12 respondent(s)
        - More damaging: 12 respondent(s)
        - No response: 1 respondent(s)
    - Ocean-caused
        - Less damaging: 1 respondent(s)
        - About the same: 8 respondent(s)
        - More damaging: 4 respondent(s)
        - No response: 12 respondent(s)
    - River-caused
        - Less damaging: 3 respondent(s)
        - About the same: 9 respondent(s)
        - More damaging: 8 respondent(s)
        - No response: 5 respondent(s)
7. What economic and/or health impacts have you seen from these types of floods? (briefly list)
8. Select ALL the resources you typically use during a flood event in regards to response and recovery in your community, county, or region
9. Select ALL the resources you typically use during a flood event in regards to response and recovery in your community, county, or region - websites or software
10. Select ALL the resources you typically use during a flood event in regards to response and recovery in your community, county, or region - field-based tools
11. Select ALL the resources you typically use during a flood event in regards to response and recovery in your community, county, or region - other
12. Select ALL the resources you typically use to seek funding for hazard mitigation planning in your community, county, or region
13. Select ALL the resources you typically use to seek funding for hazard mitigation planning in your community, county, or region - websites or software
14. Select ALL the resources you typically use to seek funding for hazard mitigation planning in your community, county, or region - field-based tools
15. Select ALL the resources you typically use to seek funding for hazard mitigation planning in your community, county, or region - other

Appendix C: Equations

Probability Distribution Density Functions

LogLogistic

$$f(x) = \frac{(\beta/\alpha)(x/\alpha)^{\beta-1}}{(1+(x/\alpha)^{\beta})^2} \tag{6}$$

where α is the scale parameter and is also the median of the distribution and β is a shape parameter.

Inverse Gaussian

$$f(x) = \sqrt{\frac{\lambda}{2\pi x^3}} exp\left[-\frac{\lambda(x-\mu)^2}{2\mu^2 x}\right] \tag{7}$$

for $x > 0$, where $\mu \geq 0$ is the mean and $\lambda \geq 0$ is the shape parameter.

Generalized Extreme Value

$$f(x) = \frac{1}{\sigma} t(x)^{\xi+1} e^{-t(x)} \tag{8}$$

where

$$t(x) = \begin{cases} (1+\xi) & if \xi(\frac{x-\mu}{\sigma}) \neq 0 \\ e^{-(x-\mu)/\sigma)} & if \xi = 0 \end{cases} \tag{9}$$

Gamma The general formula for the probability density function of the gamma distribution is

$$f(x) = \frac{(\frac{x-\mu}{\beta})^{\gamma-1} \exp{(-\frac{x-\mu}{\beta})}}{\beta\Gamma(\gamma)} \qquad x \geq \mu; \gamma, \beta > 0 \tag{10}$$

where γ is the shape parameter, μ is the location parameter, β is the scale parameter, and Γ is the gamma function which has the formula

$$\Gamma(a) = \int_0^\infty t^{a-1} e^{-t} dt \tag{11}$$

Weibull

$$f(x) = \frac{\gamma}{\alpha}(\frac{x-\mu}{\alpha})^{(\gamma-1)} \exp{(-((x-\mu)/\alpha)^{\gamma})} \qquad x \geq \mu; \gamma, \alpha > 0 \tag{12}$$

where γ is the shape parameter, μ is the location parameter and α is the scale parameter.

Birnbaum Saunders The Birnbaum-Saunders distribution is also commonly known as the fatigue life distribution. There are several alternative formulations of the Birnbaum-Saunders distribution in the literature. The general formula for the probability density function of the Birnbaum-Saunders distribution is

$$f(x) = \left(\frac{\sqrt{\frac{x-\mu}{\beta}} + \sqrt{\frac{\beta}{x-\mu}}}{2\gamma(x-\mu)} \right) \phi \left(\frac{\sqrt{\frac{x-\mu}{\beta}} - \sqrt{\frac{\beta}{x-\mu}}}{\gamma} \right) \quad x > \mu; \gamma, \beta > 0 \tag{13}$$

where γ is the shape parameter, μ is the location parameter, β is the scale parameter, φ is the probability density function of the standard normal distribution, and ϕ is the cumulative distribution function of the standard normal distribution.

Copula Functions

The families of copulas detailed here are used within this study. u_1, u_2, u_3 represent the best-fit distribution of variables while θ represents the copula's parameter value.

Gumbel Copula. The multivariate Gumbel copula takes the form,

$$C(u_1, u_2, ..., u_n; \theta) = \exp\left(-\left(\sum_{i=1}^{n} (-\ln u_i)^{\theta} \right)^{1/\theta} \right) \tag{14}$$

with parameter, $\theta \geq 1$.

The trivariate Gumbel copula takes the form,

$$C(u_1, u_2, u_3; \theta) = e^{-[(-\ln u_1)^{\theta} + (-\ln u_2)^{\theta} + (-\ln u_3)^{\theta}]^{1/\theta}} \tag{15}$$

Clayton The multivariate Clayton opula takes the form,

$$C(u_1, u_2, ..., u_n; \theta) = \left(\sum_{i=1}^{n} u_i^{-\theta} - n + 1 \right)^{-1/\theta} \tag{16}$$

with parameter, $\theta > 0$.

The trivariate clayton copula takes the form,

$$C(u_1, u_2, u_3; \theta) = \max[(u_1^{-\theta} + u_2^{-\theta} u_3^{-\theta} - 2)^{-1/\theta}, 0] \tag{17}$$

Frank Copula. The trivariate Frank copula takes the form,

$$C(u_1, u_2, u_3; \theta) = -\frac{1}{\theta} \ln \left[1 + \frac{(e^{-\theta u_1} - 1)(e^{-\theta u_2} - 1)(e^{-\theta u_3} - 1)}{(e^{-\theta} - 1)^2} \right] \tag{18}$$

Joe Copula. The multivariate Joe copula takes the form,

$$C(u_1, u_2, ..., u_n; \theta) = 1 - \left(\sum_{i=1}^{n} (1 - u_i)^\theta - \prod_{i=1}^{n} (1 - u_i)^\theta \right)^{1/\theta} \tag{19}$$

with parameter, $\theta \geq 1$.

Appendix D: Univariate Distributions Goodness-of-Fit

Northern Case Study: Precipitation Distributions Goodness-of-Fit

Distribution	NLogL	BIC	AIC	AICc
Inverse Gaussian	172.74	**352.53**	349.47	349.86
Generalized Extreme Value	**171.05**	352.69	**348.11**	**348.91**
Birnbaum Saunders	172.86	352.78	349.73	350.12
Lognormal	172.93	352.90	349.85	350.24
LogLogistic	173.52	354.10	351.04	351.43
Gamma	174.79	356.63	353.58	353.96
Rayleigh	178.04	359.61	358.08	358.21
Nakagami	177.33	361.71	358.66	359.04
Weibull	177.92	362.90	359.84	360.23
Rician	178.04	363.13	360.08	360.47
Logistic	179.00	365.05	362.00	362.38
T Location Scale	177.99	366.56	361.98	362.78
Normal	181.32	369.69	366.63	367.02
Exponential	190.52	384.57	383.04	383.17
Extreme Value	191.38	389.81	386.76	387.15

Minimum value indicating best fit is **bolded**.

Northern Case Study: Tide Level Distributions Goodness-of-Fit

Distribution Name	NLogL	BIC	AIC	AICc
Generalized Extreme Value	**-2.89**	**4.80**	**0.22**	**1.02**
LogLogistic	-0.35	6.35	3.30	3.69
Lognormal	0.32	7.70	4.65	5.03
Inverse Gaussian	0.34	7.73	4.68	5.06
Birnbaum Saunders	0.35	7.76	4.71	5.09
Gamma	1.36	9.77	6.72	7.11
Logistic	1.93	10.92	7.86	8.25
Nakagami	2.59	12.23	9.18	9.56
t Location Scale	0.96	12.50	7.93	8.73
Rician	3.89	14.83	11.78	12.16
Normal	3.95	14.94	11.89	12.28
Weibull	7.52	22.09	19.04	19.42
Extreme Value	13.41	33.88	30.82	31.21
Rayleigh	24.97	53.47	51.94	52.07
Exponential	46.86	97.25	95.72	95.85

Minimum value indicating best fit is **bolded**.

Northern Case Study: Stream Discharge Distributions Goodness-of-Fit

Distribution Name	NLogL	BIC	AIC	AICc
Gamma	**136.65**	**280.29**	**277.30**	**277.70**
Nakagami	136.84	280.68	277.69	278.09
Weibull	137.46	281.92	278.92	279.32
LogLogistic	141.03	289.06	286.07	286.47
Lognormal	141.22	289.44	286.45	286.85
Birnbaum Saunders	145.43	297.85	294.86	295.26
Generalized Extreme Value	146.71	303.90	299.41	300.24
Generalized Pareto	147.72	305.93	301.44	302.27
Exponential	165.42	334.33	332.83	332.96
t Location Scale	171.01	352.51	348.03	348.85
Logistic	191.27	389.53	386.53	386.93
Normal	196.59	400.17	397.18	397.58
Inverse Gaussian	199.12	405.24	402.24	402.64
Extreme Value	208.54	424.08	421.09	421.49
Rayleigh	263.90	531.30	529.80	529.93
Rician	263.90	534.79	531.80	532.20

Minimum value indicating best fit is **bolded**.

Central Case Study: Precipitation Distributions Goodness-of-Fit

Distribution Name	NLogL	BIC	AIC	AICc
Inverse Gaussian	**179.39**	**365.88**	**362.77**	**363.15**
Birnbaum Saunders	179.50	366.10	362.99	363.37
LogNormal	179.56	366.24	363.13	363.50
LogLogistic	180.14	367.39	364.28	364.66
Generalized Extreme Value	178.60	367.86	363.20	363.97
Gamma	181.26	369.63	366.52	366.89
Rayleigh	184.40	372.36	370.81	370.93
Nakagami	183.69	374.50	371.39	371.76
Weibull	184.27	375.66	372.55	372.92
Rician	184.40	375.92	372.81	373.18
Logistic	185.51	378.12	375.01	375.39
t Location Scale	184.69	380.05	375.38	376.15
Normal	187.67	382.45	379.34	379.71
Exponential	197.23	398.01	396.45	396.58
Extreme Value	197.75	402.61	399.50	399.87

Minimum value indicating best fit is **bolded**.

Central Case Study: Tide Level Distributions Goodness-of-Fit

Distribution Name	NLogL	BIC	AIC	AICc
Generalized Extreme Value	**-3.47**	**3.73**	**-0.94**	**-0.17**
Inverse Gaussian	-1.30	4.52	1.41	1.78
Birnbaum Saunders	-1.29	4.54	1.43	1.80
Lognormal	-1.25	4.61	1.50	1.87
Gamma	-0.59	5.93	2.82	3.20
LogLogistic	-0.47	6.17	3.06	3.44
Nakagami	0.17	7.46	4.35	4.72
Rician	1.08	9.27	6.16	6.53
Normal	1.12	9.35	6.24	6.62
Logistic	1.42	9.94	6.83	7.21
t Location Scale	1.11	12.90	8.23	9.00
Weibull	3.32	13.76	10.65	11.02
Extreme Value	7.01	21.14	18.02	18.40
Rayleigh	22.84	49.24	47.69	47.81
Exponential	45.35	94.26	92.71	92.83

Minimum value indicating best fit is **bolded**.

Central Case Study: Stream Discharge Distributions Goodness-of-Fit

Distribution Name	NLogL	BIC	AIC	AICc
Weibull	**163.97**	**335.05**	**331.94**	**332.32**
Gamma	164.37	335.86	332.75	333.12
LogNormal	165.52	338.15	335.04	335.41
LogLogistic	165.98	339.07	335.96	336.33
Nakagami	166.59	340.30	337.18	337.56
Birnbaum Saunders	166.75	340.60	337.49	337.87
Generalized Pareto	165.07	340.80	336.14	336.91
Exponential	168.80	341.16	339.61	339.73
Generalized Extreme Value	168.38	347.43	342.76	343.54
Inverse Gaussian	176.26	359.64	356.52	356.90
t Location Scale	181.73	374.12	369.46	370.23
Logistic	189.98	387.06	383.95	384.33
Normal	197.37	401.85	398.74	399.11
Extreme Value	212.06	431.23	428.12	428.50
Rayleigh	223.08	449.72	448.16	448.28
Rician	223.08	453.27	450.16	450.54

Minimum value indicating best fit is **bolded**.

Southern Case Study: Precipitation Distributions Goodness-of-Fit

Distribution Name	NLogL	BIC	AIC	AICc
Weibull	**163.97**	**335.05**	**331.94**	**332.32**
Gamma	164.37	335.86	332.75	333.12
LogNormal	165.52	338.15	335.04	335.41
LogLogistic	165.98	339.07	335.96	336.33
Nakagami	166.59	340.30	337.18	337.56
Birnbaum Saunders	166.75	340.60	337.49	337.87
Generalized Pareto	165.07	340.80	336.14	336.91
Exponential	168.80	341.16	339.61	339.73
Generalized Extreme Value	168.38	347.43	342.76	343.54
Inverse Gaussian	176.26	359.64	356.52	356.90
t Location Scale	181.73	374.12	369.46	370.23
Logistic	189.98	387.06	383.95	384.33
Normal	197.37	401.85	398.74	399.11
Extreme Value	212.06	431.23	428.12	428.50
Rayleigh	223.08	449.72	448.16	448.28
Rician	223.08	453.27	450.16	450.54

Minimum value indicating best fit is **bolded**.

Southern Case Study: Tide Level Distributions Goodness-of-Fit

Distribution Name	NLogL	BIC	AIC	AICc
Inverse Gaussian	**-0.81**	**5.19**	**2.38**	**2.83**
Birnbaum Saunders	**-0.81**	**5.19**	2.39	**2.83**
LogNormal	-0.79	5.22	2.42	2.86
LogLogistic	-0.59	5.62	2.81	3.26
Gamma	-0.51	5.78	2.98	3.42
Nakagami	-0.14	6.53	3.73	4.17
Rician	0.33	7.47	4.66	5.11
Normal	0.35	7.51	4.70	5.15
Logistic	0.35	7.51	4.71	5.15
Generalized Extreme Value	-1.20	7.81	3.60	4.52
Generalized Pareto	0.34	10.88	6.68	7.60
t Location Scale	0.34	10.89	6.69	7.61
Weibull	2.54	11.87	9.07	9.52
Extreme value	5.00	16.80	14.00	14.44
Rayleigh	25.07	53.54	52.14	52.28
Exponential	44.89	93.17	91.77	91.91

Minimum value indicating best fit is **bolded**.

Southern Case Study: Stream Discharge Distributions Goodness-of-Fit

Distribution Name	NLogL	BIC	AIC	AICc
Birnbaum Saunders	**197.05**	**400.91**	**398.11**	**398.55**
Exponential	199.01	401.42	400.02	400.16
Inverse Gaussian	197.75	402.31	399.51	399.95
LogNormal	198.12	403.05	400.25	400.69
Generalized Pareto	196.53	403.26	399.06	399.98
Gamma	198.96	404.72	401.92	402.37
Weibull	199.00	404.81	402.01	402.45
LogLogistic	199.21	405.23	402.43	402.87
Nakagami	200.27	407.34	404.54	404.99
Generalized Extreme Value	199.27	408.75	404.54	405.47
Logistic	210.88	428.56	425.76	426.21
t Location Scale	209.84	429.89	425.68	426.61
Normal	211.80	430.40	427.60	428.05
Rayleigh	215.22	433.84	432.44	432.59
Rician	215.22	437.25	434.44	434.89
Extreme Value	218.97	444.73	441.93	442.38

Minimum value indicating best fit is **bolded**.